

Middle-Late Quaternary Palaeoclimate Variability from Lacustrine Deposits in the Nefud Desert, Northern Arabia

Highlights

- Palaeoclimatic reconstruction of four palaeolake records from Northern Arabia
- Wet phases reported during MIS 11/9, 7, 5, 3 and the Early Holocene
- Lake and wetland formation coincides with human occupation of the region

1 **Middle-Late Quaternary Palaeoclimate Variability from Lake and**
2 **Wetland Deposits in the Nefud Desert, Northern Arabia**

3

4 **Ash Parton^{1,2}, Laine Clark-Balzan³, Adrian G. Parker¹, Gareth W. Preston¹, Wing Wai**
5 **Sung⁴, Paul S. Breeze⁵, Melanie J. Leng⁶, Huw S. Groucutt^{7,8}, Tom S. White⁹, Abdullah**
6 **Alsharekh¹⁰, Michael D. Petraglia⁸**

7

8 ¹ Department of Social Sciences, Oxford Brookes University, Headington Campus, Gypsy Lane,
9 Oxford, OX3 0BP, United Kingdom

10 ² Mansfield College, University of Oxford, Oxford, OX1 3TF, United Kingdom

11 ³ Albert-Ludwigs-Universität Freiburg, Freiburg im Breisgau, Baden-Württemberg, Germany

12 ⁴ Department of Life Sciences, The Natural History Museum, Cromwell Road, London, SW7 5BD,
13 United Kingdom

14 ⁵ Department of Geography, King's College London, Strand, London, WC2R 2LS, United Kingdom

15 ⁶ NERC Isotope Geosciences Laboratory, British Geological Survey, Nottingham, NG12 5GG, United
16 Kingdom, and Centre for Environmental Geochemistry, University of Nottingham, Nottingham, NG7
17 2RD, United Kingdom

18 ⁷ School of Archaeology, Research Laboratory for Archaeology and the History of Art, University of
19 Oxford, Oxford, OX1 2PG, United Kingdom

20 ⁸ Max Planck Institute for the Science of Human History, Kahlalsche Strasse 10, D-07745 Jena,
21 Germany

22 ⁹ Department of Zoology, University of Cambridge, Downing Street, Cambridge, CB2 3EJ, UK

23 ¹⁰ Department of Archaeology, King Saud University, Riyadh, Saudi Arabia

24

25 **Abstract**

26 Records of former lake and wetland development in present day arid/hyper-arid
27 environments provide an important source of information for palaeoclimatic and
28 palaeoenvironmental studies. In Arabia, such records are typically confined to
29 eccentricity-modulated insolation maxima, and are often spatially and temporally

30 discontinuous. Here we present records from a single locality in Northern Arabia of
31 wetter interludes during both global interglacial and glacial conditions, providing a
32 unique opportunity to examine the nature of these events in a common setting. At
33 Jubbah, in the southern Nefud Desert, lake and wetland deposits reveal the repeated
34 formation of a water body within a large endorheic basin over the past ca. 360 kyr.
35 Lake/wetland formation occurred during MIS 11/9, 7, 5, 3 and the early Holocene,
36 assisted by local topographic controls, and spring recharge. Palaeoenvironmental and
37 palaeoecological data reveal the existence of a large still water body formed during
38 either MIS 11 or 9 (ca. 363 ka), and basin wide alluviation followed by lake formation
39 during MIS 7 (ca. 212 ka). During MIS 5e (ca. 130 ka) a large freshwater lake
40 occupied the basin, while during MIS 5a (ca. 80 ka) the basin contained a shallow
41 wetland and freshwater lake complex. Lake/wetland formation also occurred during
42 early MIS 3 (ca. 60 ka), at the Terminal Pleistocene-Holocene transition (ca. 12.5 ka),
43 and the early-middle Holocene (ca. 9-6.5 ka). Phases of lake and wetland
44 development coincided with human occupation of the basin during the Middle
45 Palaeolithic, Epipalaeolithic and Neolithic periods, highlighting the significance of
46 the region for early demographic change.

47

48 **Keywords:** *Pleistocene; Holocene; Paleoclimatology; Paleolimnology; Arabia;*

49 *Stable isotopes; Luminescence Dating; Diatoms; Palaeolithic; Neolithic*

50

51 **Corresponding Author:** Ash Parton (aparton@brookes.ac.uk)

52 Department of Social Sciences, Oxford Brookes University, Headington Campus, Gipsy Lane, Oxford,

53 OX3 0BP, United Kingdom

54

55

56

57 **1. Introduction**

58 Palaeoenvironmental records of lake and wetland development in desert regions
59 provide an important means to better understand subtropical climate dynamics and the
60 response of arid zones to climate change. Water bodies that form in these regions are
61 sensitive to climatic changes (Battarbee, 2000), and constitute excellent records of
62 hydrological responses to both regional and global climate variability (e.g. Trauth et
63 al., 2003). In addition, arid regions such as the Saharo-Arabian desert belt have been
64 the setting for major environmental changes throughout the course of human history,
65 with large scale variations in water availability potentially driving the evolutionary
66 and techno-cultural trajectories of human populations throughout the Pleistocene and
67 Holocene periods (e.g. Staubwasser and Weiss, 2006; Trauth et al., 2007; Shea, 2008;
68 Grove, 2012; Maslin et al., 2014; Groucutt et al., 2015a). Palaeoenvironmental and
69 palaeoecological data derived from these records, therefore, also provide an important
70 means to explore the connections between environmental change and past
71 demographic variability.

72

73 Palaeolake development throughout Arabia is indicative of high amplitude
74 oscillations in the dominant atmospheric systems that drive climate change across the
75 peninsula. Situated within the subtropical Sahara-Arabian-Thar desert belt, the
76 Arabian Peninsula lies at the interface of several complex and seasonally variable
77 rain-bearing systems. Rainfall derived from the African and Indian Ocean monsoons,
78 Mediterranean cyclones and Red Sea synoptic troughs, has contributed to large-scale
79 hydrodynamic changes during the Pleistocene and Holocene periods (e.g. Engel et al.,
80 2011; Fleitmann et al., 2011; Rosenberg et al., 2013; Parton et al., 2015a; 2015b;
81 Preston et al., 2015). These include the widespread activation of major drainage
82 systems, lake and wetland development, groundwater and aquifer recharge,
83 speleothem and spring formation, and alluvial fan activation. Precipitation increases

84 have also been accompanied by pervasive vegetative development and an associated
85 increase in landscape stability. While our understanding of when and to what extent
86 rainfall from each of these systems drove such changes remains fairly limited,
87 palaeoenvironmental reconstructions from palaeolake and palaeowetland records have
88 been used to develop a broad framework for establishing long-term, orbital-scale
89 climate variability across the region.

90

91 Lacustrine and palustrine carbonates from the deserts of the Nefud, Rub' al Khali
92 (Empty Quarter) and Wahiba (e.g. Radies et al., 2005; Parker et al., 2006; Rosenberg
93 et al., 2011; 2013; Engel et al., 2011; Matter et al., 2015; Groucutt et al., 2015b;
94 Preston et al., 2015), predominantly comprise relatively thin sequences (i.e. 1-3 m) of
95 interstratified calcareous silts, sands and marls, relating to key pluvial periods such as
96 MIS 5e (ca. 130-120 ka), 5c (ca. 105-95 ka), 5a (ca. 85-75 ka) and the early-mid
97 Holocene period (ca. 11-6 ka). With the exception of a few records dated to early MIS
98 3 (e.g. Parton et al., 2013; Hoffmann et al., 2015; Matter et al., 2015; Jennings et al.,
99 2016), lake and wetland formation overwhelmingly coincides with eccentricity-
100 modulated insolation maxima. However, few records display evidence of repeated
101 interglacial lake formation within the same basin, while none provide records of
102 markedly wetter conditions during both glacial and interglacial periods.

103

104 The absence of continuity in Arabian lake records through glacial-interglacial cycles,
105 and/or their lack of sensitivity to 'weaker' pluvials recently identified in fluvial-
106 alluvial archives (Parton et al., 2015a), is likely determined by a combination of
107 specific climatic and geomorphological controls. In the first instance, the
108 predominance of high potential evaporative losses in Arabia (up to 3000 mm yr⁻¹) is
109 such that precipitation must increase dramatically for substantial water bodies to
110 form. This has typically occurred during interglacials. Indeed, Pleistocene-Holocene

111 lake formation across Arabia corresponds closely with speleothem growth, which has
112 occurred predominantly during interglacials (e.g. Fleitmann et al., 2003; 2011). For
113 wetter periods that occur during drier global glacial conditions, such as the brief wet
114 phase at the onset of MIS 3 (ca. 60-55 ka), high levels of evaporation combined with
115 generally low rainfall levels may have been insufficient for significant lake formation
116 or speleothem growth. This situation would also be exacerbated by the nature of
117 rainfall across the peninsula, which would have likely comprised seasonally regulated
118 high magnitude storm events.

119

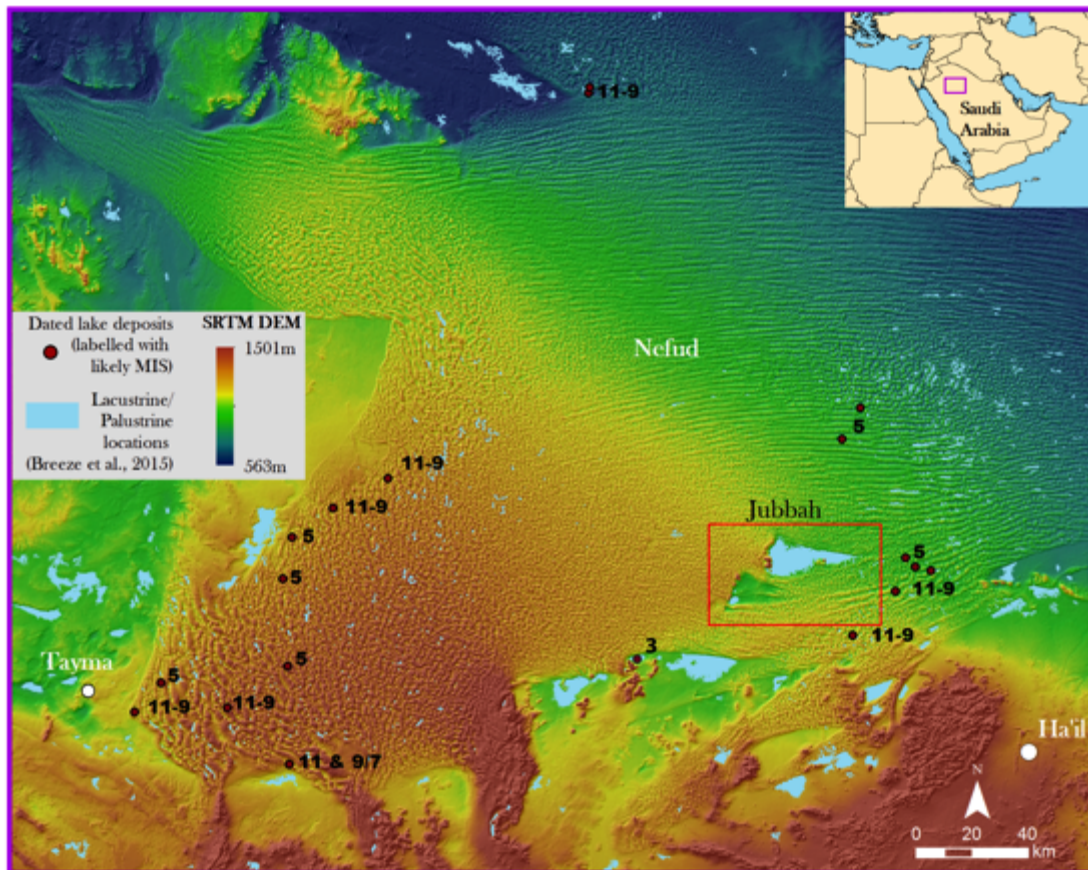
120 Secondly, geomorphological settings exert significant control over both water body
121 formation and archive preservation in dryland lakes. In some arid basins where the
122 primary source of inflow is from the continuous discharge of allogenic rivers in more
123 humid climatic zones, large perennial freshwater lakes may form. In Arabia, however,
124 the major drainage systems that feed large basins such as Mundafan in the southern
125 Rub' al-Khali and Tayma in northwest Arabia (Fig. 1), lie broadly within the same
126 arid climatic belt, with only relatively minor (~150 mm) differences in annual rainfall
127 between the basins and their montane headwaters. In addition, basin morphology
128 plays a critical role in determining the permanency of a lentic water body through the
129 provision of accommodation space. Palaeolake deposits in Arabia are mostly situated
130 within shallow endorheic and/or deflationary basins. These may be interdunal
131 depressions (e.g. Whitney et al., 1983; Parker et al., 2004; 2006; Radies et al., 2005;
132 Rosenberg et al., 2013; Preston et al., 2015) or spatially extensive but flat depressions
133 in which topographic depth is insufficient to enable water retention during periods of
134 higher evaporation (e.g. McClure, 1976; Rosenberg et al., 2011a; Engel et al., 2011;
135 Groucutt et al., 2015b). Similarly, there is a general paucity of lacustrine records that
136 preserve more than one or two lake expansion phases within the same depression. As
137 such, in order for lentic water body formation to persist beyond peak wet periods in

138 Arabia, a unique set of geomorphic controls need to be in place to overcome high
139 evaporative losses (e.g. Parton et al., 2013). Given these issues and the seasonality of
140 the climate, all lake and wetland records from Arabia should be expected to reflect
141 astatic water levels with one or more major evaporitic phases.

142

143 Here we present for the first time, a unique record of repeated long-term lake and
144 wetland development spanning multiple interglacials from a large basin within the
145 Nefud Desert, Northern Saudi Arabia. These comprise two ~9 m, one ~4 m and one
146 ~2 m thick sequences composed of interstratified clays, marls, diatomites, silts,
147 gypsum and sands. Multiproxy analyses have in turn revealed a detailed record of
148 hydroclimatic change during the Middle-Late Pleistocene and Early Holocene
149 periods. Our findings indicate the repeated development of an extensive water body
150 over the past ca. 360 kyr during both global glacial and interglacial periods, due to
151 favourable geomorphic controls and shallow groundwater. In addition, lake/wetland
152 development is seen to correspond with the repeated hominin/human occupation of
153 the region.

154



155

156 **Figure 1: Map showing location of the Jubbah basin within the Nefud, including**
 157 **estimated extent of lacustrine/palustrine deposits (Breeze et al., 2015), and**
 158 **location of dated Pleistocene lake deposits reported by Rosenberg et al. (2013)**
 159 **and Stimpson et al. (2016), giving corresponding Marine Isotope Stage of lake**
 160 **formation.**

161

162 **2. Background**

163 *2.1. Physical Setting*

164 The Nefud Desert (Fig. 1) is situated within a depression that covers ~375,000 km²
 165 and dips gently to the northeast. The sand sea itself covers some 57,000 km² between
 166 Jawf and Ha'il regions, with an average elevation of ~900 m asl (Vincent, 2008). The
 167 desert sands have accumulated to a depth of up to ~100 m, and extend east to the ad-
 168 Dahna sand belt, through which they are linked to the Rub' al-Khali in the south. In
 169 the north and south, the Nefud is characterised by complex linear dune ridges oriented

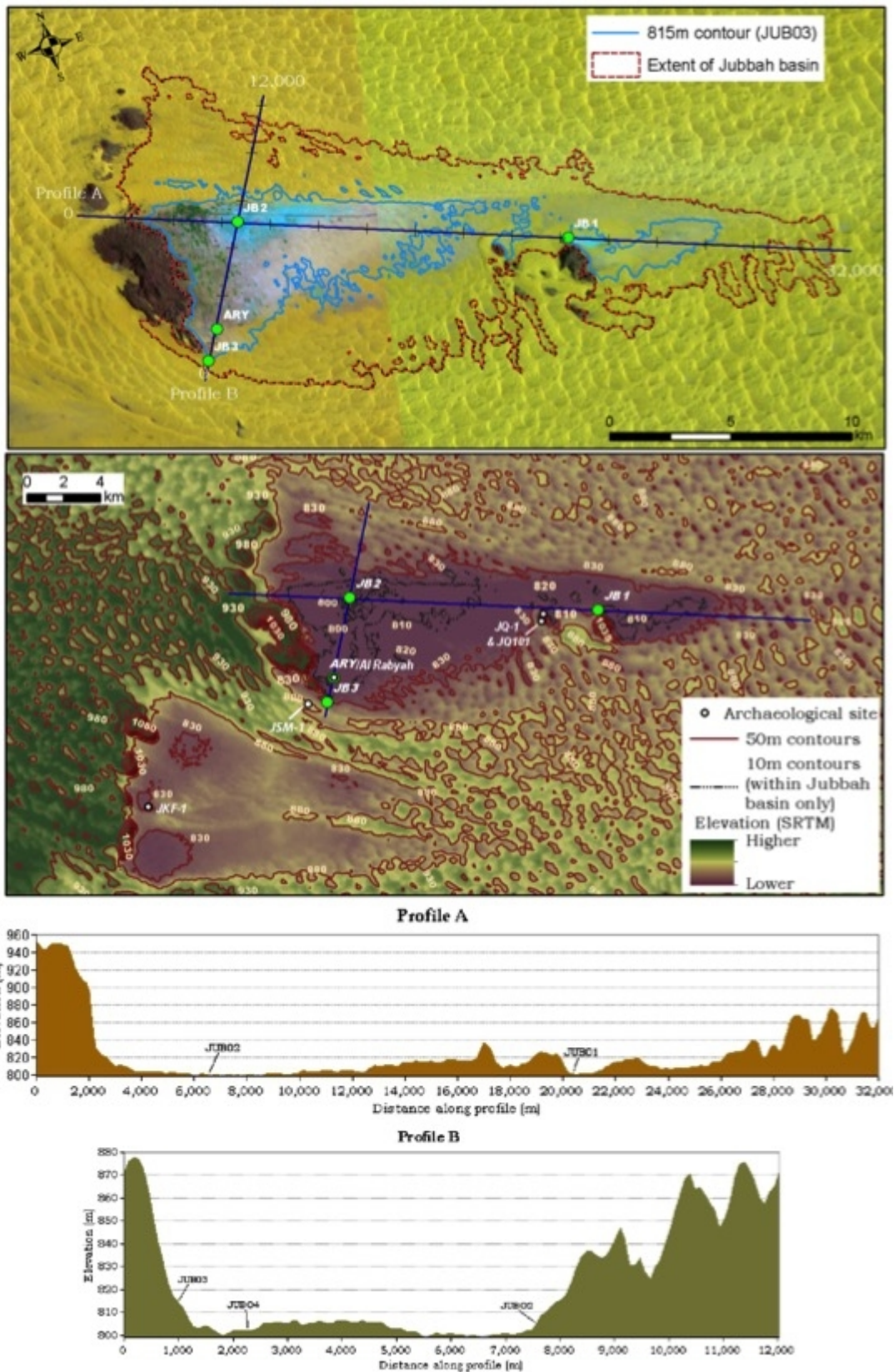
170 parallel to the prevailing wind, while central and western regions are predominantly
171 composed of compound barchanoid dunes. The underlying depression is situated
172 within the Interior Shelf; an outcrop of Palaeozoic to Lower Cretaceous detrital rocks
173 that surround the Arabian Shield in a semi circle from Tabuk and the Widyan basin
174 margin in the north, to the Wajid basin in the southeast. The major structural elements
175 of the northern parts of the shelf comprise vast outcrops of Cambro-Ordovician
176 sandstones, which dip gently towards the east-northeast, and occasionally outcrop
177 from their covering of Quaternary sediments (Wagner, 2011).

178

179 Groundwater within the region is derived from the Saq aquifer, which extends across
180 375,00 km² in Saudi Arabia and Jordan (Alsharhan et al., 2001), forming the major
181 aquifer for both countries. Groundwater occurs within the Saq under both confined
182 and unconfined conditions, and flows east towards the Jubbah region under an
183 average hydraulic gradient of 0.017 (Hussein et al., 1992; Barthélemy et al., 2007).

184 While more saline at greater depth, groundwater within the aquifer is fresh and of
185 good quality at the margin of sandstone outcrops, extending considerable distances
186 from the areas beneath the overlying confining strata (Lloyd and Pim, 1990).

187 Presently, aquifer recharge occurs through high intensity storms, and resulting in ~3-
188 11 mm of recharge per year across the region (Fisk and Pim, 1985; UN-ESCWA and
189 BGR, 2013). Runoff is minimal, however, infiltration of rainfall through the dunes
190 may be significant. Within the region, annual rainfall of ~80 mm per year will
191 produce approximately 20 mm of water recharge to local and shallow aquifers
192 through the dunes (Dincer et al., 1974), allowing seepage into topographic
193 depressions, facilitating vegetation growth and by extension, increasing landscape
194 stability. During previous periods of substantially higher rainfall, infiltration through
195 the dunes surrounding depressions would have been a major contributor to lake water
196 recharge, while also extending the recharge phase beyond that of the rainy season.



197

198 **Figure 2: Figure showing map of the Jubbah basin and location of the four**
 199 **studied sections; (JB1-3 & ARY), and previously reported archaeological sites**
 200 **and palaeoenvironmental records (JQ-1 (Petraglia et al., 2012), JQ-101**

201 (Crassard et al., 2013), JKF-1 (Groucutt et al., 2015c) and JSM-1 (Groucutt et
202 al., 2017)).

203

204 2.2. *The Jubbah Basin*

205 The Jubbah basin is the largest endorheic depression in the south-central Nefud (Fig.
206 1 & 2). It lies approximately 80 km northwest of Hail, and ~50 km inside the southern
207 border of the sand sea. The basin is situated at ~800 m asl and is bordered on its
208 northern and southern sides by compound barchanoid dunes that extend up to 80 m
209 above the basin floor. At the western margin of the basin, Jebel Umm Sanman rises to
210 ~200 m above the basin, its presence sheltering the depression from the eastward
211 transport and accumulation of aeolian sand. The overall maximum extent of the
212 Jubbah depression is ~32 km (west-east) by ~12 km (north-south), covering a total
213 area of ~177 km². This is defined by the areas facing downslope into the basin, the
214 surrounding dune faces, and exposed surfaces underlying the dunes that form the
215 basin floor. The latter accommodates two distinct basins within the 815 m contour
216 range, which denotes the maximum elevation at which preserved lacustrine/wetland
217 deposits are recorded within the basin. No preserved shoreline deposits were observed
218 within the basin. This is likely due to the substantial urban and agricultural
219 development that has taken place across the Jubbah basin, combined with burial by
220 later phases of dune reactivation along the fringes of the depression. To the west, a
221 larger basin directly sheltered by Jebel Umm Sanman is ~44 km². To the east, the
222 smaller Jebel Ghawtah range rises to a height of 1082 m asl, and has similarly led to
223 the development of a small deflationary basin approximately 7.8 km². Both ranges
224 have Saq sandstone at their base and Tabuk sandstone near their summit (Bramkamp
225 et al., 1963). Throughout the basin, groundwater lay near to the modern surface as
226 recent as the late 19th Century (e.g. Blunt, 1881), with the town of Jubbah forming an
227 oasis that has been repeatedly occupied over recent centuries and millennia (Jennings

228 et al., 2014). Due to modern agricultural practices, however, water now lies at a depth
229 of at least ~50m, with recent groundwater depletion models (Al Salamah et al., 2011)
230 suggesting that drawdown may currently be as great as 1 m per year. At the eastern
231 end of the basin, fossil spring outcrops are reported by Crassard et al. (2013), which
232 represent areas of focused discharge of the Saq aquifer.

233

234 Pleistocene and Holocene lacustrine and palustrine records have been reported from
235 the Jubbah region, often associated with archaeological assemblages (Fig. 2). Lower
236 Palaeolithic assemblages have been identified at Jubbah and in other nearby basins,
237 yet they currently lack precise chronological attribution (Shipton et al., 2014).

238 Petraglia et al. (2011; 2012) describe a perched sequence of isolated palaeosols and
239 lacustrine sediments at the site of Jebel Qattar-1 (Fig. 2) that are stratigraphically
240 bounded by aeolian sediments and dated to MIS 5 and MIS 7, with both periods
241 having associated Middle Palaeolithic archaeological material. The MIS 7 assemblage
242 currently represents the earliest dated Middle Palaeolithic material from the Arabian
243 Peninsula. The site of JSM-1, located just south of Jebel Umm Sanman (Fig. 2),
244 produced a Middle Palaeolithic assemblage, which probably dates to late MIS 5
245 (Petraglia et al., 2012). A small lake is also reported from an adjacent basin at Jebel
246 Katefeh (Petraglia et al., 2012; Groucutt et al., 2015c), which represents a phase of
247 human occupation associated with Middle Palaeolithic technology. Reported ages
248 from the site indicate a possible MIS 5a age (ca. 90-85 ka) for lake formation,
249 however, a notable population of younger grains (ca. 50 ka) highlight the potential for
250 an early MIS 3 age of the site. Indeed, hominin occupation of the Nefud during early
251 MIS 3 (ca. 60-50 ka) is reported from the Al Marrat basin, which is located ~50 km
252 southwest of Jubbah (Fig. 1) (Jennings et al., 2016). If the MIS 5 age estimates are
253 correct, then the technological differences between JKF-1, JSM-1 and JQ-1, suggest
254 considerable demographic and behavioural complexity within the Jubbah basin at this

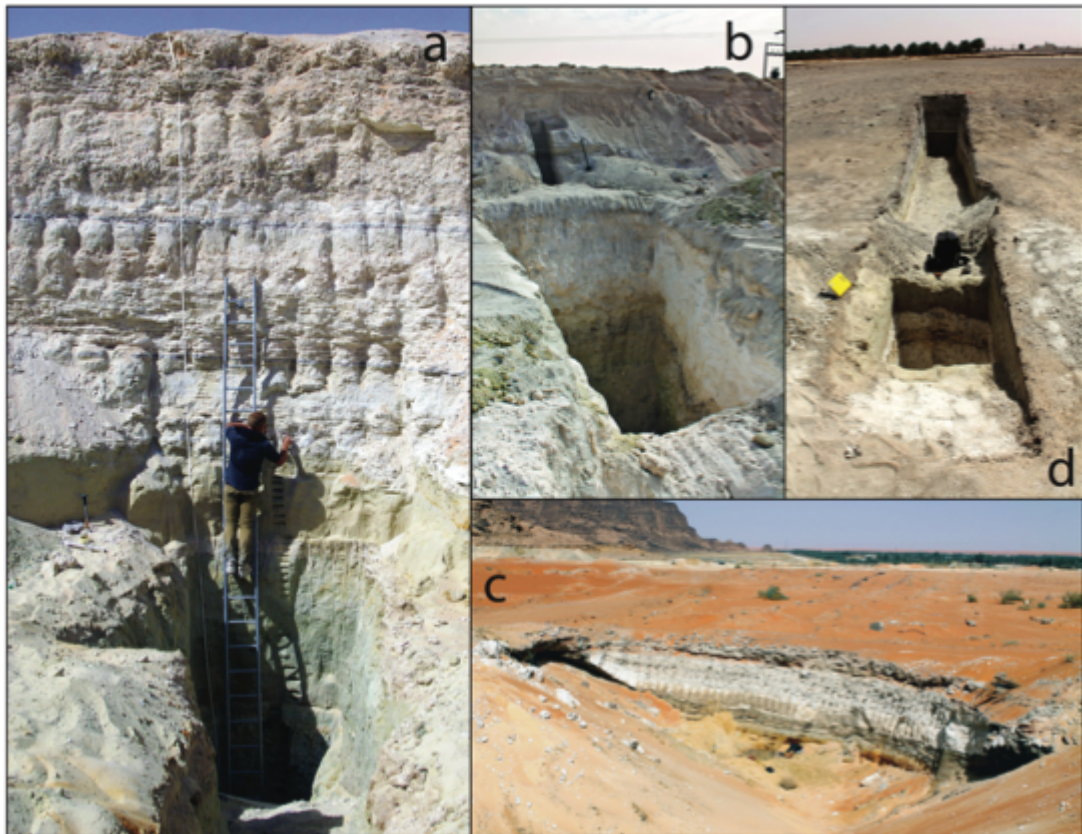
255 time (Scerri et al., 2015). Given recent interest in processes such as the dispersal of
256 *Homo sapiens* out of Africa and admixture between *Homo sapiens* and Neanderthals,
257 refining the chronology of archaeological and palaeoenvironmental sites at Jubbah
258 remains a key task.

259

260 Evidence for Holocene-age lake formation within the Jubbah basin is reported by
261 Crassard et al. (2013), who describe a small sequence of lacustrine silts featuring
262 plant macrofossils and reed stems, indicative of shallow water conditions, dated to ca.
263 9-8 ka. It was argued by Crassard (2013) that the lithic assemblage at the adjacent JQ-
264 101 archaeological site (Fig. 2), demonstrated similarities (particularly in arrowhead
265 forms) with the Pre Pottery Neolithic, previously known from the Fertile Crescent. At
266 the site of Al Rabyah (Fig. 2), Hilbert et al. (2014) report a sequence of palustrine-
267 type sediments dated to ca. 6.5 ka, which reflect shallow but perennial and well-
268 vegetated conditions, underlain by deposits indicative of deeper water conditions
269 dated to at least ca. 12 ka. A lithic assemblage located in sandy sediments between
270 these two phases of lake formation at Al Rabyah is similar to Epipalaeolithic
271 assemblages known from the Levant, particularly those assigned to the Geometric
272 Kebaran. Ostensibly the findings from the Nefud agree with the wider picture of lake
273 formation across Arabia, with the timing of lake development corresponding to
274 eccentricity-paced insolation maxima. These appear to have allowed cultural
275 connections with the Levant to the north, but the precise form these interactions took
276 remains unclear and a key topic for future research. The extent to which demographic
277 and behavioural changes in the Holocene represent autochthonous developments,
278 cultural diffusion, and population dispersal has been debated (see e.g. Guagnin et al.,
279 2015), and a key area of resolution rests on the recovery of securely dated
280 archaeological, palaeontological and palaeoenvironmental data from this region.

281

282 A report by Garrard et al. (1981) describes a ~26 m interstratified sequence
283 comprising seven major sedimentary units composed of clays, carbonates and sands,
284 which were deposited directly on top of the Saq sandstone. The lowermost units were
285 ~12 m of clays, overlain by ~12 m of calcareous diatomaceous silts. The uppermost
286 units described in the study were positioned on the banks of a shallow drainage runnel
287 adjacent to Jebel Umm Sanman, located approximately 1.5 km west of the deep
288 sequence described above. These comprised an interstratified sequence of sand, silt
289 and diatomite dated by ^{14}C to 25,630±430 B.P., overlain by a palaeosol dated to
290 6,685±50 B.P. (Garrard et al., 1981). The findings presented here comprise the first
291 detailed palaeoenvironmental and palaeoecological analysis of the deposits initially
292 described by Garrard, along with a substantially revised and detailed chronology
293 based on OSL and radiocarbon dating techniques (see Clark-Balzan et al., 2017 for
294 further details of the chronology presented here). In addition, this study provides an
295 important framework for the demographic changes reported in the aforementioned
296 archaeological studies.
297



298

299 **Figure 3: Photographs showing the excavated sections at JB1 (a), JB2 (b), JB3 (c)**
300 **and Al Rabyah (ARY) (d).**

301

302

303

304 **3. Methods and Materials**

305 Four sedimentary sequences comprising palaeolake and palaeowetland deposits were

306 excavated within the Jubbah basin (Fig. 2 & 3). At the eastern end of the basin

307 (28.020381 N, 41.095013 E), a sequence approximately 0.3 km from the base of Jebel

308 Ghawtar (JB1) was excavated to a depth of 9.5 m. At the western end (28.020993 N,

309 40.955891 E), a sequence approximately 3 km from the base of Jebel Umm Sanman

310 was excavated to a depth of 8.5 m (JB2). A third sequence (JB3), situated

311 approximately 0.3 km from the base of Jebel Umm Sanman (27.974871 N, 40.925377

312 E) was excavated to a depth of 4 m. New data and an additional OSL age (Clark-

313 Balzan et al., 2017) is also reported from a fourth sequence (Al-Rabyah - ARY),

314 which is situated ~1 km north of JB3 and previously described by Hilbert et al.
315 (2014). Samples were extracted from all sites for
316 palaeoenvironmental/palaeoecological laboratory analyses. A more detailed
317 multiproxy analysis was conducted at the deepest and most stratigraphically complex
318 section, JB1.

319

320 Analyses of organic carbon (LOI_{org}) and carbonate content (LOI_{carb}) were conducted
321 following the standard procedure described by Dean (1974) and Heiri et al. (2001).
322 Environmental magnetic susceptibility measurements were determined following
323 Dearing (1999). Samples for bulk (<63 μm fraction) inorganic carbonate isotope
324 analysis ($^{18}\text{O}/^{16}\text{O}_{\text{carb}}$ and $^{13}\text{C}/^{12}\text{C}_{\text{carb}}$) of the JB1 sequence were prepared following
325 standard off line vacuum extraction procedures (e.g. Lamb et al. 2000) and all
326 measurements made using a VG Optima mass spectrometer. The stable isotope
327 analyses were conducted at the NERC Isotope Geosciences Laboratory, Keyworth,
328 Nottingham. Conductivity measurements were made using a Jenway Model 470
329 Conductivity Meter. For laser granulometry of the <2 μm sediment component,
330 samples were disaggregated in de-ionised water with 5% sodium hexametaphosphate,
331 and analysed using a Malvern Mastersizer 2000.

332

333 Samples for diatom analysis were prepared using the methods outlined by Renberg
334 (1990). 30% H_2O_2 and 5% HCl were added to samples to digest organic material and
335 remove calcium carbonate. After heating the samples were diluted with distilled water
336 and stored in the refrigerator. The samples were rinsed daily and allowed to settle
337 overnight for four days. The slides were air-dried at room temperature in a dust free
338 environment prior to mounting with Naphrax diatom mountant. Diatom taxonomy
339 followed Krammer and Lange-Bertalot (1986; 1988; 1991a; 1991b), Pouličková, and
340 Jahn (2007), Saros and Anderson (2015), and Nakov et al. (2015). Ideally 300

341 hundred valves should be enumerated for a representative sample; however, in certain
342 circumstances, i.e. for samples with low abundances, a modified enumeration strategy
343 can be used to enable fewer valves to be counted (Battarbee et al., 2001). Samples
344 with fewer than 100 valves were omitted from subsequent analyses, as these do not
345 provide a representative sample since most change in species occurs between 0 and
346 100 valves. Correspondence Analysis was used to examine the prevalent trends in the
347 assemblage after Detrended Correspondence Analysis showed that the gradient length
348 was greater than 1.5 SD units using the program CANOCO version 4.5 (Ter Braak
349 and Prentice, 1988). Theorised zones of sedimentation and palaeoenvironmental
350 change at the sites were derived from all palaeoenvironmental proxy data using the
351 optimal sum of the squares partitioning with the program ZONE (Lotter and Juggins,
352 1991; *unpublished*). Statistically significant zones were deduced by comparison with
353 the Broken Stick model using the program BSTICK version 1 (Bennet, 1996).

354

355

356 3.1 *Chronology*

357 Radiocarbon dating was attempted at JB1. Two charred plant fragments collected in
358 the field (2.58 m, 2.65-2.68 m) and five bulk sediment samples from horizons
359 determined to be rich in organic carbon (0.40-0.50 m, 0.85-0.90 m, 3.05-3.15 m, 3.40-
360 3.50 m, 4.26-4.28 m) were submitted to the Oxford Radiocarbon Accelerator Unit
361 (ORAU) (for protocols see Bronk Ramsey et al. (2002) and Bronk Ramsey et al.
362 (2004)). Of these, only the unidentified plant fragment at 2.65-2.68 m could be dated
363 after pretreatment. This sample was dated to 7925 ± 45 ^{14}C years BP, which is
364 calibrated for a final age of 8980-8609 cal BP at the 95.4% range via the IntCal13
365 calibration curve (Reimer et al., 2013) using OxCal v4.2 (Bronk Ramsey, 2009).
366 Factors that might have influenced the use of this radiocarbon date as an estimator for
367 the depositional age of the surrounding sediment were considered (Clark-Balzan et

368 al., 2017), including bioturbation, overestimation of age due to residence times before
369 burial (affecting woody plants; see Oswald et al., 2005), underestimation due to
370 inherited geological carbon (affecting submerged and emergent plants; see Marty and
371 Myrbo, 2014) due to nearby carbonates and Saq aquifer waters ($20,400 \pm 500$ ^{14}C
372 years, Thatcher et al., 1961), and contamination by modern carbon. We consider that
373 this sample provides a reliable depositional age.

374

375 A combined quartz OSL and feldspar post IR-IRSL (290 °C) (pIRIR₂₉₀) luminescence
376 dating study was implemented for these sites. For full details of this project, see
377 Clark-Balzan (2016) and Clark-Balzan et al. (2017); pertinent details are summarized
378 here. Samples for luminescence dating were collected by hammering sections of
379 plastic or metal tubing into the cleaned section face, after which these were capped.
380 The full depth of the section was systematically sampled at a resolution of one sample
381 per approximately every 0.50 m (JB1—JB3) or higher (ARY). Sand-rich layers were
382 preferentially targeted, followed by carbonate-rich/gypsum-poor layers; highly
383 gypsiferous units were sampled only if no other suitable unit was available near the
384 chosen depth. Water content samples were also collected, and gamma spectrometer
385 measurements were made on site for all samples except ARY-OSL4. Mineral
386 extraction followed procedures given in Hilbert et al. (2014) for the quartz samples
387 from ARY, and slightly altered procedures in Clark-Balzan (2016) and Clark-Balzan
388 et al. (2017) designed to reduce the proportion of gypsum in the measured extracts.
389 Quartz D_e 's were measured via a blue-light OSL SAR protocol (Murray and Wintle,
390 2000; 2003) incorporating recycled, zero-dose, and IR depletion steps (Duller, 2003).
391 Feldspar D_e 's were measured via the pIRIR290 protocol (Thiel et al., 2011a, b),
392 which also incorporates recycled and zero-dose steps. Supplemental experiments
393 included a dose recovery (12 aliquots for $D_e + 4$ for bleaching residual) and fading
394 characterization (Huntley and Lamothe, 2001; Auclair et al., 2003). Additionally,

395 pIRIR290 D_e 's were measured from 20 aliquots of a modern aeolian surface sample
396 to check for an unbleachable residual, and IR₅₀ and pIRIR₂₉₀ residuals were calculated
397 by comparing feldspar and quartz D_e 's from five ARY samples order to examine
398 geological signal inheritance. DRAC (Durcan et al., 2015) was used to calculate dose
399 rates: alpha (for unetched quartz and all feldspars), beta, and gamma (only ARY-
400 OSL4) dose rates were calculated from elemental concentrations determined via ICP-
401 MS.

402

403 The number of samples and the minerals measured for dating the sequences described
404 here are summarized thus:

- 405 • Al Rabyah (ARY): two quartz ages (plus four from Hilbert et al., 2014), five
406 feldspar ages for residual estimation
- 407 • JB1: one quartz, five quartz + feldspar, three feldspar; two additional
408 elemental concentration samples
- 409 • JB2: six quartz, one feldspar; four additional elemental concentration samples
- 410 • JB3: three quartz, one quartz + feldspar

411

412 Luminescence D_e distributions, dose rate assessments, and age-depth relationships
413 were thoroughly examined. Both quartz OSL and feldspar pIRIR290 protocols seem
414 to provide accurate assessments of D_e , based on rejection criteria and D_e 's and similar
415 studies from the same region (for quartz) and a dose recovery experiment (feldspar).
416 Quartz and feldspar ages, too, are congruent for multiple samples from JB1, though
417 pIRIR₂₉₀ residuals are also apparent. Two samples dated via quartz are suspected to
418 be partially bleached after inspection of D_e distributions based on overdispersion and
419 skewness, while feldspar residuals calculated from ARY provide evidence for a non-
420 systematic geological signal inheritance of up to ca. 50 Gy. We did not see any
421 evidence for physical mixing of grains or, surprisingly, systematic underestimation of

422 quartz D_e 's due to saturation effects (cf. Groucutt et al., 2015b; Rosenberg et al.,
423 2011a, b). Fading experiments for the feldspars showed only low levels of fading,
424 which are expected to be laboratory artifacts. Examination of age-depth inversions,
425 comparison of the radiocarbon age and bracketing OSL ages, uranium concentrations
426 (up to 45.4 ppm), and thorium/uranium ratios, however, led to the conclusion that
427 dose rates were overestimated for a number of samples from carbonate-rich levels.
428 These samples are likely to suffer both from disequilibrium in radioisotope decay
429 chains and post-depositional uranium enrichment via carbonate re-precipitation
430 (Faure, 1986; Krbetschek et al., 1994; Olley et al., 1996; Dill, 2011). This is
431 particularly a problem when dose rates are calculated from elemental concentrations
432 as they have been in this study, due to the assumptions underlying the conversion
433 factors (Guérin et al., 2011). No constraints on the timing of the uranium enrichment
434 could be given; therefore the ages could not be modelled to account for this. Instead,
435 all of the evidence was considered, and the ages shown in Table OSL1 were judged to
436 be the most reliable based on the characterization of the units, the elemental
437 concentrations, and the age-depth relationships.

438
439

440 **Table 1: Reliable ages from the luminescence dating study of Clark-Balzan et al.**
441 **(2017) for ARY, JB1, JB2, and JB3. Quartz luminescence measurements**
442 **(excluding ARY-OSL4) were made upon unetched quartz (125-180 μm , 2 mm**
443 **aliquot diameter); for ARY-OSL4, etched quartz (180-255 μm , 4 mm aliquot**
444 **diameter) was used in order to be directly comparable with results from Hilbert**
445 **et al. (2014). Feldspar pIRIR290 measurements are reported from 180-255 μm**
446 **grains, 1 mm aliquot diameter. See text and Clark-Balzan et al. (2017) for**
447 **further details. Note that the depth of OSL samples given for JB3 include 0.7 m**
448 **of disturbed surface that are not shown in Figures 4 and 8.**

449

450

451

452

Field Code	Lab Code	Depth (m)	Mineral	Measured (# aliquots)	Accepted (# aliquots)	Overdispersion (%)	D _e (Gy)	D _r (Gy ka ⁻¹)	Age (ka)
ARY-OSL4	X6141	0.45	Q	15	14	19.21 ± 4.00	9.22 ± 0.50	1.44 ± 0.05	6.4 ± 0.4
JB1-OSL5	X 6250	4.51	F	10	10	19.43 ± 6.79	357.06 ± 28.46	4.86 ± 0.23	73.4 ± 6.8
JB1-OSL8	X 6253	5.50	F	10	8	43.49 ± 11.9	302.45 ± 48.79	2.23 ± 0.16	135.8 ± 23.9
JB1-OSL13	X 6258	9.00	F	10	5	47.96 ± 18.18	889.16 ± 209.98	4.30 ± 0.20	206.6 ± 49.7
JB2-OSL1	X 6216	0.77	Q	18	12	14.43 ± 4.62	5.93 ± 0.32	0.69 ± 0.03	8.6 ± 0.6
JB2-OSL4	X 6219	3.94	Q	20	7	18.24 ± 6.62	9.78 ± 6.62	1.14 ± 0.05	8.6 ± 0.8
JB2-OSL14	X 6228	8.65	F	8	6	54.11 ± 16.17	844.81 ± 189.89	2.35 ± 0.16	359.4 ± 84.3
JB3-OSL1	X 6231	1.20	Q	18	14	52.18 ± 10.31	61.63 ± 8.79	1.10 ± 0.04	56.2 ± 8.3
JB3-OSL2	X 6232	1.67	Q	18	14	48.08 ± 9.90	55.00 ± 6.32	0.83 ± 0.03	66.3 ± 8.0
JB3-OSL3	X 6233	2.07	Q	18	10	62.22 ± 14.42	83.60 ± 16.75	0.83 ± 0.03	100.5 ± 20.5
JB3-OSL4	X 6234	2.50	Q	18	11	30.83 ± 7.77	94.98 ± 9.64	1.26 ± 0.05	75.3 ± 8.1

453

454

455 4. Results

456 Zonation of key depositional phases is shown along with multiproxy

457 palaeoenvironmental and palaeoecological records in Figures 5-9. Due to insufficient

458 carbonate material, isotope values were not obtained from units 1-6 at JB1. A total of

459 84 diatom species were identified at JB1, and only species with an abundance of over

460 12% (14 taxa) are shown. At ARY, a total of 76 diatom species were identified with

461 an abundance of 7% (15 taxa) shown. A notable feature of the sequences at JB1 and

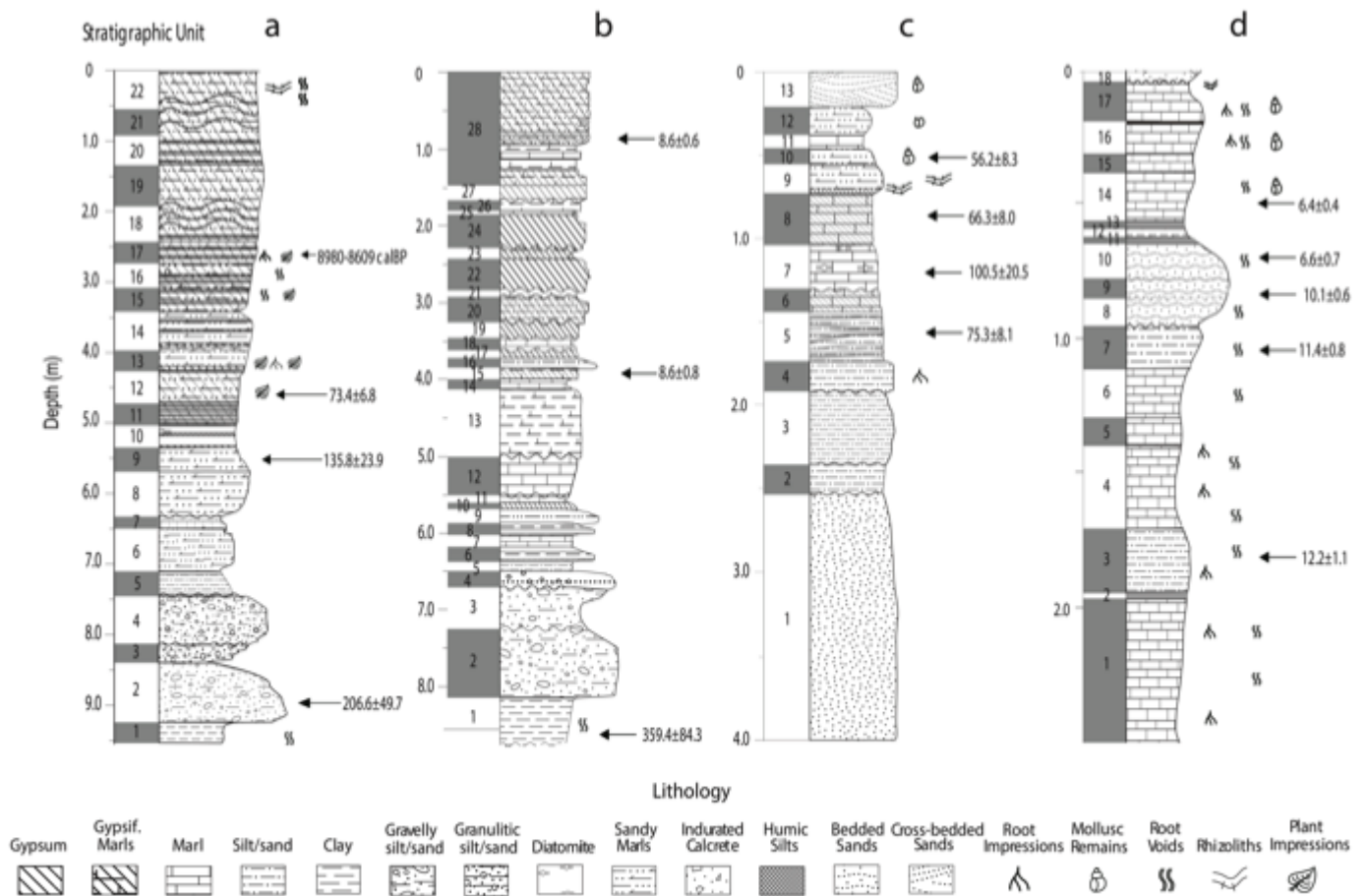
462 JB2 is their depth (9.5 m and 8.5 m respectively) compared to those previously

463 reported from Arabia, which generally range from 0.5-2.0 m. In addition, unlike those

464 previously reported from the Nefud, the sequences display a highly complex

465 stratigraphy featuring interstratified clays, gravels, marls, gypsum, diatomite, silts and

466 sands.



470 **Figure 4: Stratigraphy of sequences JB1 (a), JB2 (b), JB3 (c) and ARY (d),**
 471 **showing reliable ages derived from each section. Note, for illustrative purposes,**
 472 **section depths do not utilise the same scale.**

473

474 4.1. Middle and Late Pleistocene Proxy Records

475 The chronology for each sequence was predominantly constructed from ages derived
 476 directly from waterlain sediments, and are therefore representative of wetter periods.

477 Phases of Middle and Late Pleistocene sedimentation within the Jubbah basin are
 478 reported from JB1, JB2 and JB3, the oldest of which (359.4±84.3 ka) is recorded at

479 JB2 (JB2-OSL14). Due to substantial error ranges on this date, this phase may be

480 attributable to increased rainfall during either MIS 9 (ca. 337-300 ka) or MIS 11 (424-

481 374 ka). While this phase of lake formation is most likely indicative of one of these
482 wet phases, the overlapping error range with both MIS 11 and 9 currently prohibits a
483 firm assignment to either period. The unit is free from large gravel clast inclusions,
484 interbedding or bioturbation, indicating undisturbed still water deposition and the
485 dissolution of underlying sandstone bedrock material. Notably similar sedimentary
486 characteristics are observed at the base of JB1 (Unit 1), possibly reflecting
487 contemporaneous formation. At JB1, lower gravelly silt/sands are likely to be older
488 than 206.6 ± 49.7 ka (JB1-OSL13), though a minimum age of 151.9 ± 36.0 ka
489 calculated due to the existence of an outlying, younger aliquot cannot be entirely
490 ruled out (see Clark-Balzan et al., 2017). Given these ages and the corresponding
491 errors, we suggest that this phase of sedimentation corresponds with increased
492 regional rainfall during MIS 7. This depositional phase is characterised by the
493 mobilisation and deposition of weathered material from the adjacent Jebel Ghawtar.
494 As before, similar gravelly sediments are observed overlying the lowermost clayey
495 deposits at JB2, which again may reflect the contemporaneous deposition of these
496 facies across the wider basin. A lack of reliable ages from this unit at JB2, however,
497 prevents confirmation of this. In both sequences a sharp, uniform bounding surface
498 with no evidence of scouring separates gravel and clay units, which likely reflects a
499 depositional hiatus between the units.

500

501 At both JB1 and JB2, gravelly/granulitic sediments gradually progress into a sequence
502 of interbedded silt-sands and finely laminated marls. Zonation at JB1 (Fig. 5), and the
503 presence of a diffuse contact with the underlying gravels, suggests that these may
504 reflect a continuation of sedimentation during MIS 7. No further robust Pleistocene
505 ages were retrieved from JB2, however, an age of 135.8 ± 23.9 ka was obtained from
506 lacustrine material at JB1 (JB1-OSL8), which is taken to reflect an intensification of
507 rainfall during MIS 5e. Zonation at JB1 suggests a marked change in deposition at 6.5

508 m (Unit 7), which we suggest reflects the onset of MIS 5e at ca. 130 ka. The basal
509 marls of Zone II are finely laminated, loosely consolidated and friable, with some
510 minor signs of haloturbation at lateral extensions of the unit, and with occasional
511 gypsum lenses within Units 8 and 9, consistent with rapid drying phases. The upper
512 section of Zone II is characterised by well-developed marls, which transition sharply
513 into a well developed gypsum layer. This is overlain by Zone III, which is comprised
514 of a thick diatomite layer featuring low $\delta^{18}\text{O}$ values, high silt and carbonate content
515 with a band of humic silts at the lower contact. This likely represents the
516 diatomaceous marls previously reported by Garrard et al. (1981) and dated by ^{14}C to
517 $25,630\pm 430$ B.P. Diatoms assemblages within this unit reveal a diverse range of taxa
518 with high relative abundances of benthic/epipellic taxon *Staurosirella pinnata* var.
519 *pinnata*, *Staurosirella lapponica*, *Campylodiscus clypeus*. The occurrence of
520 *Campylodiscus* and well-developed laminae throughout marl units are characteristic
521 of fluctuating water levels at the site at this time. However, particularly high CA Axis
522 1 sample scores and the dominance of *Cyclotella distinguenda* and *Lindavia comensis*
523 throughout this zone, also reveal a large shift in the planktonic: benthic ratio
524 indicative of rising water levels and water body expansion.

525

526 A gradual shift towards more benthic and epipellic conditions at the top of Unit 10 at
527 JB1 reflect a change from deep to shallow water conditions. Benthic and
528 tycho planktonic taxa within Unit 11 (e.g. *Nitzschia dissipata*, *Fragilaria famelica*) are
529 typical of shallow, yet freshwater eutrophic lakes. Increased sand influx, higher $\delta^{18}\text{O}$
530 and $\delta^{13}\text{C}$ values (+6.08‰ and -4.9‰ respectively) as a result of evaporation (Leng
531 and Marshall, 2004), decreased organic content and numerous well-developed
532 gypsum lenses, also reflect a move to drier conditions and greater sensitivity to short-
533 term P/E changes. At this point, lake water residence time was likely substantially
534 reduced, with high evaporative losses and lower lake levels insufficient to dampen the

535 effects of short-term climatic variations (e.g. Lamb et al., 2000; Leng and Marshall,
536 2004). It should be noted, however, that contributions from groundwater and/or
537 infiltration from water bodies higher up the flow path make interpretation of the
538 isotopic signal problematic, producing potentially unrepresentative values than would
539 normally be produced from meteoric waters alone.

540

541 A feldspar age of 73.4 ± 6.8 ka within Zone IV of JB1 (Unit 12) is consistent with
542 increased regional rainfall during MIS 5a at ca. 80 ka, although it may be slightly
543 older, as a subtraction method intended to circumvent environmental dose rate
544 changes yields a low-precision estimate of 117.1 ± 51.2 ka. This phase of
545 sedimentation comprises sandy marls characterised by generally high organic carbon
546 content, numerous plant impressions and low $\delta^{18}\text{O}$ and $\delta^{13}\text{C}$ values. A successive
547 peak in clay content corresponds to numerous calcretised plant remains, whilst a
548 progressive enrichment of $\delta^{18}\text{O}$ (-5.5‰ to $+2.8\text{‰}$) and $\delta^{13}\text{C}$ (-11.1‰ to -4.3‰)
549 values indicates a move towards shallower palustrine conditions. The presence of a
550 dark, humic layer at 4.20 m supports the latter supposition and reflects the formation
551 of black mats related to groundwater discharge, which generally form in wetland
552 environments. The presence of *Rhopalodia constricta* indicates a shift to more
553 brackish conditions, possibly reflecting a move to drier conditions at the end of MIS
554 5a. The occurrence of benthic species *Nitzschia dissipata*, *Rhopalodia constricta* and
555 *Nitzschia angustata* also suggests shallower water depth. The unit is also
556 characterised by high gypsum content; however, this is blocky, poorly developed and
557 highly variable across profile, suggesting it may be diagenetic in origin, having
558 formed at depth following the downward percolation of water during a subsequent
559 wet phase. Other ages retrieved from Units 10-14 at JB1 seem to be significantly
560 affected by uranium enrichment; therefore these are not considered reliable.
561 Subtraction ages suggest that these units are likely to represent MIS 5 deposits,

562 though it is possible that feldspar residuals have caused age overestimation and an
563 MIS 3 age is certainly plausible (see Clark-Balzan et al., 2017).

564

565 A similar quartz age of 75.3 ± 8.1 ka is reported from Zone III at JB3 (JB3-OSL4). A
566 stratigraphically reversed age of 100.5 ± 20.5 in Unit 7 (JB3-OSL3) was recorded at
567 the interface between Zones III and IV at the site, and we suggest that both of these
568 ages likely reflect an increase in rainfall during MIS 5a between ca. 85-75 ka. Given
569 the higher elevation of JB3 (Fig. 2) and its distinctly basinal cross-sectional profile, it
570 is likely that the sequence represents the formation of a smaller, isolated interdunal
571 water body. This may have been contemporaneous with water body formation
572 recorded at JB1; however, an absence of strict age controls inhibits this interpretation.
573 At JB3, the three samples collected within carbonate-rich layers (JB3-OSL1—JB3-
574 OSL3) yielded quartz D_e distributions with higher overdispersion values than
575 expected based on results from nearby sites. We attribute the skewed distribution of
576 JB3-OSL2 to partial bleaching and apply a minimum age model to calculate the D_e ,
577 and suggest that the symmetric but scattered distributions of samples JB3-OSL1 and
578 JB3-OSL4 are more likely to relate to microdosimetric variation in the alpha and beta
579 dose rates. The numerous shell fragments throughout the upper units may provide
580 high and low dose rate regions (Kaufman et al., 1996); high dose rate minerals such as
581 zircons are known to be present (Garzanti et al., 2013), and the unusually
582 consolidated carbonates may have provided shielding to some grains (Nathan et al.,
583 2003; 2008).

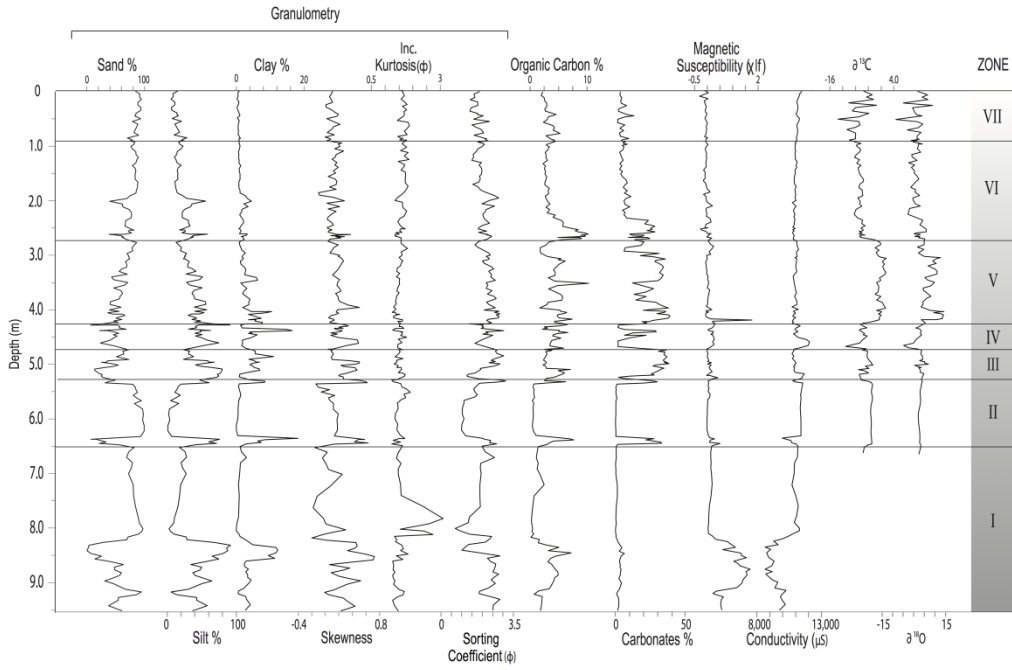
584

585 Unlike the other sequences within the Jubbah basin, JB3 indicates lake formation
586 during global glacial conditions. Quartz ages from Zones IV and V of 66.3 ± 8.0 and
587 56.2 ± 8.3 respectively are consistent with lake formation during early MIS 3.
588 Sedimentary characteristics and proxy values suggest a shift in lake water levels

589 during this period, characterised by alternating gypsiferous marls, diatomite and well-
590 developed gypsum layers. Numerous rhizoliths, dark humic bands and highly variable
591 proxy values throughout the zone indicate fluctuating water levels at the site, followed
592 by eventual lake desiccation. Conspicuous throughout Zone V are high concentrations
593 of shells and shell fragments. These assemblages are predominantly composed of
594 bivalves, notably *Cerastoderma* sp. and *Mytilopsis* sp, together with low
595 concentrations of hydrobiid gastropods (*Hydrobia* cf. *lactea*) and occasional ostracods
596 (*Cyprideis torosa*). The assemblage is typical of lagoons or estuaries, and is thus
597 indicative of brackish conditions. The valves of *C. torosa* are smooth, indicating
598 salinities higher than ~5 ‰. Both *Cerastoderma* and *Mytilopsis* are tolerant of a wide
599 range of salinities, but are most often found in brackish waters. These bivalves can
600 attain very high densities, in the case of *Cerastoderma* exceeding 13,000 individuals /
601 m² (Legezynska and Wiktor, 1981), accounting for the richness of the samples
602 recovered from the JB3 sequence.

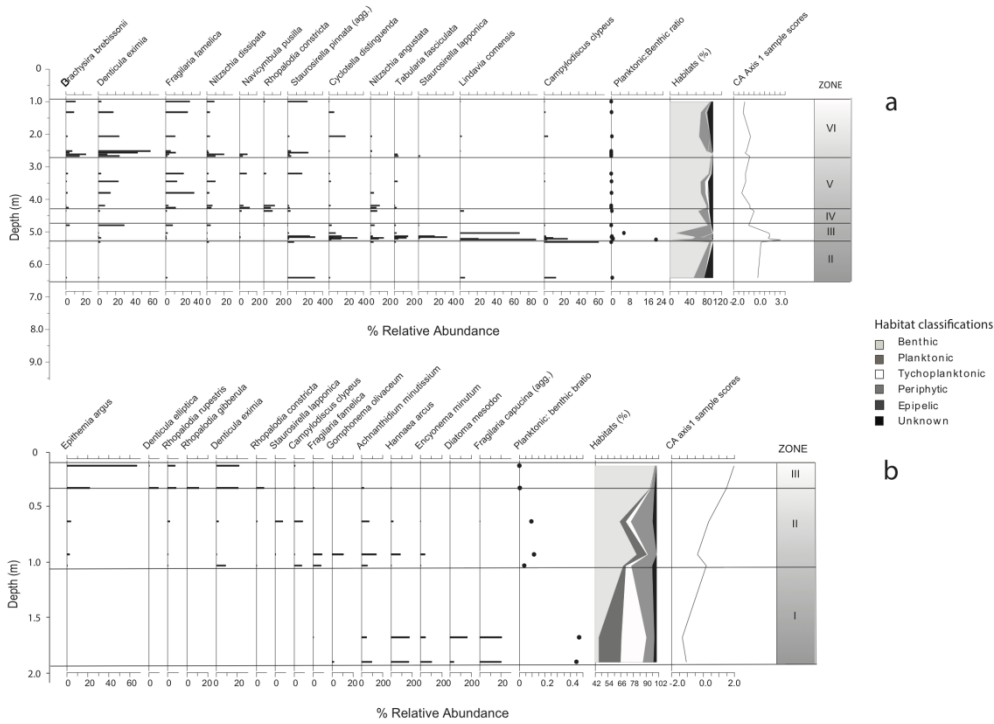
603

604

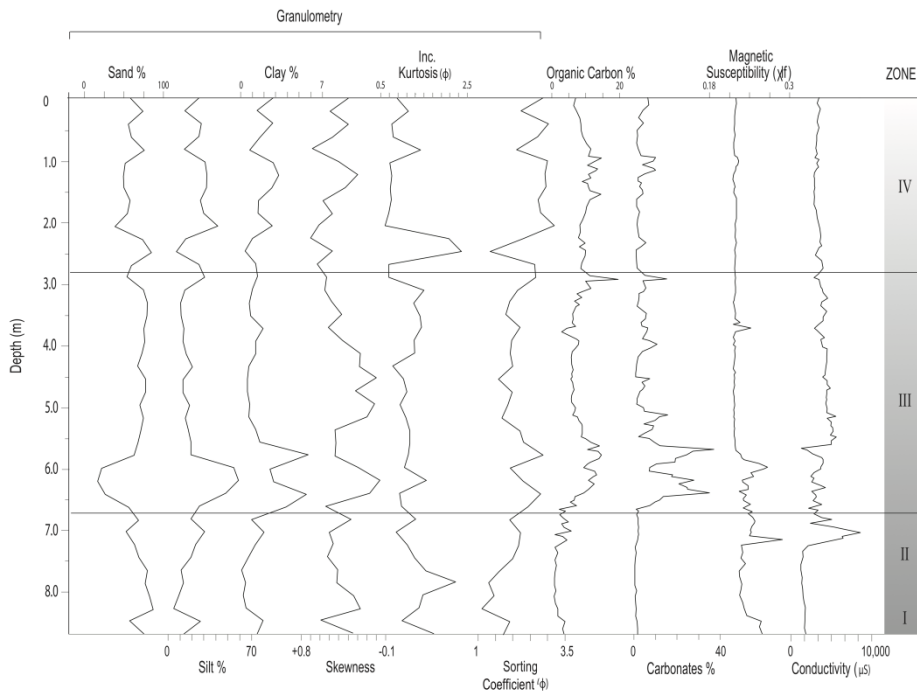


606 **Figure 5: Multiproxy record from JB1.**

607

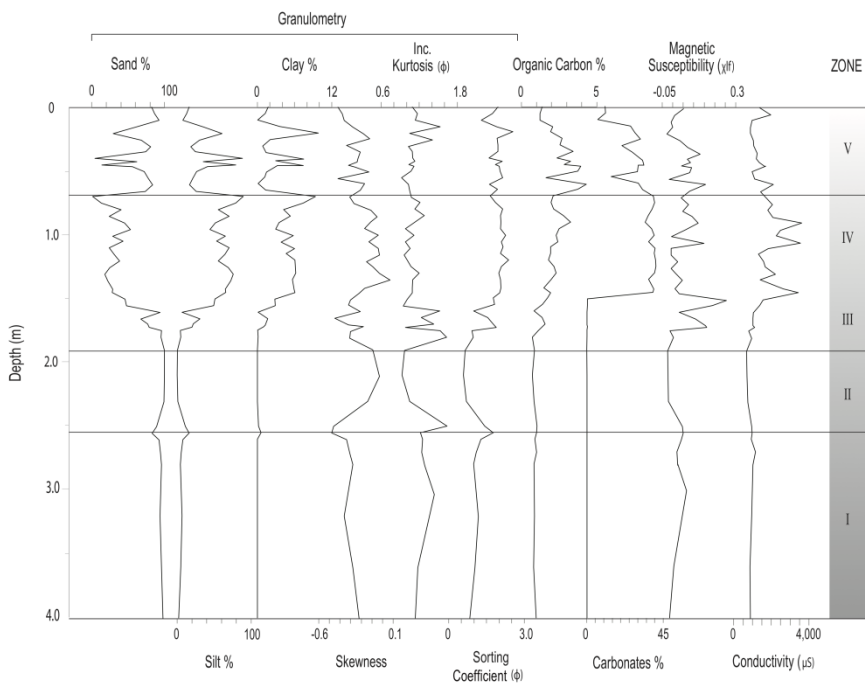


609 **Figure 6: Diatom records from JB1 & ARY.**



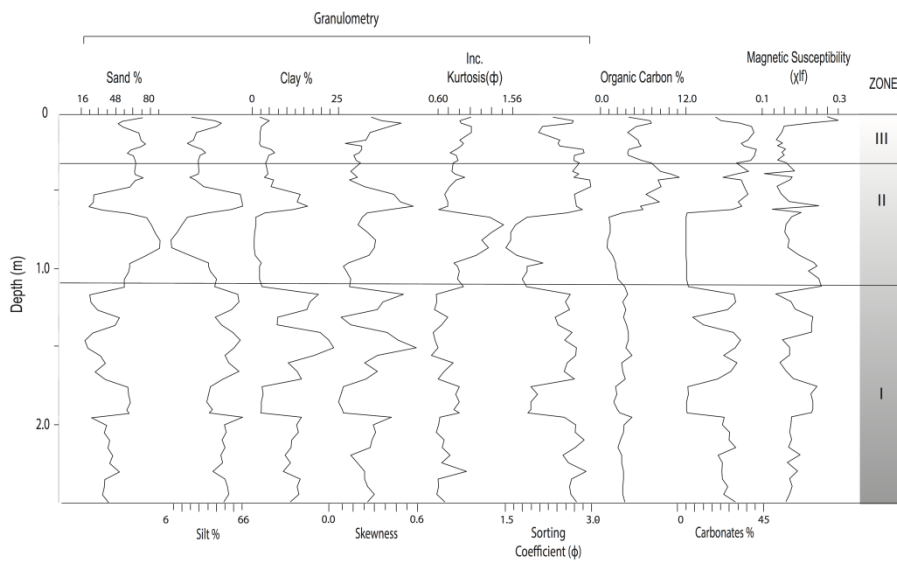
611 **Figure 7: Multiproxy record from JB2.**

612



614 **Figure 8: Multiproxy record from JB3.**

615



617 **Figure 9: Multiproxy record from ARY.**

618

619 *4.2. Terminal Pleistocene and Holocene Proxy Records*

620 Terminal Pleistocene-age deposits at Al Rabyah (ARY) comprise a series of low,
 621 inverted relief mesas capped by heavily indurated calcretes. The lowermost of these
 622 (Zone I) are composed of a thick sequence of marls featuring numerous root voids
 623 (Fig. 9), which transition sharply into moderately well sorted sands (Unit 3),
 624 suggesting a lowering of lake waters and an influx of aeolian material after 12.2 ± 1.1
 625 ka. This corresponds well with an age from the uppermost Zone IV at JB2 (Fig. 7),
 626 where a quartz age of 12.0 ± 1.1 ka is derived from a well-developed gypsum layer
 627 overlying marls. Diatom assemblages bracketing Unit 3 at ARY reveal a dominance
 628 of *Hannaea arcus*, *Fragilaria capucina* and *Diatoma mesodon*, with a high ratio of
 629 planktonic taxa, and high abundances of tychoplanktonic species indicative of deeper,
 630 fresh waters immediately before and after ca. 12 ka, with low nutrient concentrations
 631 and little organic pollution (Fig. 6). Following a subsequent phase of expansion at
 632 ARY (Units 4-6), lake waters at the site appear to contract once again between around

633 11.4±0.8 ka to 6.6±0.7 ka, which is marked by increased sand influx and a decline in
634 the planktonic: benthic ratio.
635
636 This is followed by a period of lake expansion from 6.5±0.5 ka, marked by the
637 deposition of dark, humic silts. Diatom assemblages during this period are comprised
638 of benthic taxa including *Denticula eximia*, *Fragilaria famelica*, *Rhopalodia*,
639 *Epithemia argus* and *Achnanthis minutissimum*, with a large decline in the
640 planktonic: benthic ratio and a change in the CA Axis 1 sample scores. There is
641 sparse ecological information on *Denticula eximia* although the genus *Denticula*
642 occurs in diverse environments from those that are carbonate-rich with moderate
643 conductivity to oligotrophic lakes. The presence of *Epithemia argus* and *Rhopalodia*
644 within the upper units of ARY is indicative of nutrient-poor conditions, as these
645 species may cohabit with nitrogen-fixing cyanobacteria enabling them to become
646 abundant in low nitrogen conditions (Spaulding and Metzeltin, 2011; Meyers, 2014).
647 Salinity levels also appear to have been relatively low during this period, since
648 previous palaeoecological data from ARY confirm the predominance of freshwater
649 conditions at the site during this time (Hilbert et al., 2014). Evidence from JB1 (Fig. 5
650 and 6) also indicates the presence of an early Holocene water body in the Jubbah
651 basin. A radiocarbon age of 8980-8609 cal BP was retrieved from charred plant
652 fragment material deposited within finely interdigitated marls and dark organic silts
653 featuring numerous plant and root remains. This agrees well with quartz ages of
654 8.6±0.6 (JB2-OSL1) and 8.6±0.8 (JB2-OSL4) derived from gypsiferous marls at JB2
655 (Fig. 7), which is also coincident with the deposition of dark, humic silts. We propose
656 that the upper ages from JB2 are reliable as they are indistinguishable at one sigma
657 uncertainty. There is also a substantial hiatus in sedimentation between JB2-OSL4 (at
658 ca. 4 m) and the underlying units when D_e values below and above this point are
659 compared.

660

661 Proxy values during the early Holocene (Zone VI) at JB1 are somewhat invariant with
662 respect to other zones, however, notable increases in silt, organic carbon and
663 carbonates occur in Unit 17, corresponding with numerous root and plant impressions,
664 indicative of fluctuating shallow water palustrine conditions in the basin during this
665 time. $\delta^{18}\text{O}$ and $\delta^{13}\text{C}$ values display minor fluctuations throughout Zone VI, however,
666 values are notably lower than Zone V, suggesting a phase of increasing groundwater
667 discharge from ca. 9 ka. Diatoms assemblages indicate that the prevalent species
668 during this period are benthic *Denticula exima*, *Brachysira brebissonii*, *Nitzschia*
669 *dissipata* and *Fragilaria famelica*, which are reflected by the low planktonic: benthic
670 ratio indicating shallower waters. *Denticula eximia*, *Nitzschia dissipata* and
671 *Fragilaria famelica* occur in nutrient rich freshwater whereas *Brachysira brebissonii*,
672 is common in moderately acidic (pH 4.7-5.8) to oligotrophic–mesotrophic lakes (i.e.
673 5.7-13.2 TP $\mu\text{g/L}$; Hamilton, 2010). However, high relative abundances of *Cyclotella*
674 *distinguenda*, and the recurrence of *Lindavia comensis* suggest the return of some
675 planktonic species. *Campylodiscus clypeus* also returns, highlighting increased
676 alkalinity within the lake.

677

678 Gypsum development is conspicuous throughout the upper ~3 m at both JB1 and JB2;
679 both of which feature long, needle-like prismatic crystals interdigitated with finely
680 laminated sandy marls. Such growth typically occurs in a pure supersaturated,
681 aqueous solution (i.e. water column), and although it is likely that some post-
682 depositional crystal growth may also have occurred, laminations are generally well
683 preserved, indicating that this is minimal. The presence of interdigitated wavy
684 laminations of marls and gypsum throughout the upper ca. 2 m of JB1 may be
685 indicative of seasonal lake level changes or subaerial aeolian scour. The prevalence of
686 shallow, seasonally astatic water levels featuring regular evaporitic phases is also

687 supported by large shifts in $\delta^{18}\text{O}$ and $\delta^{13}\text{C}$ values throughout the upper ~ 1 m at JB1 (–
688 9.3‰ to +8.2‰ and –13.5‰ to –1.4‰ respectively).

689

690

691 **5. Discussion**

692 *5.1. Controls on Lake Formation and Wetland Development in the Jubbah Basin*

693 The Jubbah basin records exhibit exceptional sedimentary depths in comparison to
694 other lake records from Arabia, and are currently unique in recording water body
695 formation within the same basin during both glacial and interglacial periods. We
696 suggest that this is the result of specific geomorphological controls, which have
697 facilitated the repeated formation of a water body in an oasis setting over the past ca.
698 360 kyr. The presence of sandstone outcrops has sheltered the basin from dune
699 encroachment, providing the necessary accommodation space for water body
700 formation. Lake and wetland development would have also been driven by
701 groundwater recharge from the Saq aquifer through focussed recharge from springs,
702 such as those identified near the base of Jebel Qatar (i.e. JQ-101 (Crassard et al.,
703 2013)). As such, rainfall changes in the Saq sandstone recharge area to the west of the
704 region may at times have played a more important role in the formation of water
705 bodies within the basin than local precipitation. Given the moderately long (100-300
706 km) flow paths to the recharge area, however, it should be expected that there might
707 have been a considerable lag between any climatic variation recorded at Jubbah, and
708 spring discharge response. Unfortunately, while the ages reported here for increased
709 rainfall occur in line with other records from the region, the associated errors prohibit
710 further comment on this potential lag. It is likely that such recharge events were
711 episodic, however, and that groundwater recharge may have extended the period
712 through which water entered the basin beyond wet periods.

713

714 In addition, infiltration of precipitation through the surrounding dunes, including
715 water contained within perched water bodies, will have also played an important role
716 in lake water recharge. The surrounding deep (up to 60 m thick) dunes absorb and
717 retain even minor levels of precipitation below the evaporation zone, with
718 approximately 25% of rainfall effectively infiltrating into depressions down through
719 the sand (e.g. Dincer et al., 1974). It should be noted that the underlying bedrock
720 depression might in fact continue beneath the surrounding dunes for an unknown
721 distance, hence accumulating infiltration from a large area of the dune field and
722 supporting the presence of a local perched aquifer system at Jubbah, however, the
723 extent of the underlying depression remains uncertain. While the density of vegetation
724 within the surrounding dune field would have been greater during wetter periods,
725 moisture losses due to transpiration by plants may have only played a minor role in
726 the overall water balance of the dunes. As such, it is likely that the areal extent of
727 water bodies within the Jubbah basin was determined by the balance between spring
728 discharge, evaporative losses, and marginal seepage into the dry (unsaturated) dune
729 sand sediments.

730

731 It is important to note that there is considerable contention surrounding the usage of
732 the term 'lake', and a strict definition with respect to arid regions such as Arabia, is
733 lacking. The criteria set out by Enzel et al. (2012; 2015), namely that wetlands
734 comprise 'marshy or shallow water environments' and lakes 'open water bodies' is
735 based upon typical geomorphic environments, depositional and erosional shoreline
736 features, basin sediments and biological remains of both types in arid regions (Engel
737 et al., 2017). However, these criteria apply predominantly to arid landscapes
738 dominated by structural forms, as opposed to interdunal water bodies in soft sand
739 seas. A lack of features such as shorelines is problematic in soft sediment areas,
740 particularly when factors such as human development and dune reactivation along the

741 fringes of interdunal basins are considered (e.g. Engel et al., 2017). Unfortunately,
742 there is little clarification as to the hydrological and hydrographic criteria such as
743 water depth, spatial extent, trophic ecology, or seasonal/interannual response that
744 would otherwise distinguish one type of water body from another. Indeed, the lower
745 limit size of standing (lentic) water bodies, which qualify as ‘lakes’, may be as low as
746 0.01-0.1 km² (Engel et al., 2017). When considering the residence time of such water
747 bodies, a distinction is made between lakes as being permanent (year round, persisting
748 for years to centuries), and wetlands as being ephemeral (i.e. seasonal). In this
749 respect, previous findings from Al Rabyah (ARY) at Jubbah (Hilbert et al., 2015) and
750 Tayma (Engel et al., 2012; Ginou et al., 2012), support the notion of permanent water
751 bodies in the region during the early Holocene, while faunal remains such as fish and
752 tortoise from Ti’s al Ghadah in the western Nefud (Thomas et al., 1998; Rosenberg et
753 al., 2013) point towards similar permanency during Pleistocene pluvial periods. As
754 such, while some contention continues to surround this issue, we believe that the
755 apparent perennial nature of these water bodies is nonetheless indicative of a
756 markedly increased precipitation regime (albeit greatly facilitated by groundwater
757 discharge), which was sufficient to overcome evaporative losses and allow lake
758 formation.

759

760 *5.2. Phases of Lake Formation and Wetland Development*

761 Increased precipitation occurred in line with interglacials MIS 11 or 9, 7, 5 and 1,
762 with further lake development occurring during early MIS 3. At 359.4±84.3 ka,
763 sedimentation within the basin was characterised by a thick sequence of green clayey
764 silt/sands, formed by the weathering of silicate material from the Saq sandstone and
765 long-term accumulation under still water conditions. In addition, seasonal infiltration
766 and groundwater recharge would have led to sub-surface weathering, in particular
767 oxidation and carbonate dissolution, leading to the accumulation of insoluble clays in

768 the lowest areas of the basin (e.g. Wood and Osterkamp, 1987). The homogeneity,
769 thickness and distribution of these facies across the basin at both JB1 and JB2 suggest
770 that a large lentic water body occupied the basin during this time. While this broadly
771 concurs with other studies from the region for both MIS 11 and MIS 9 (e.g.
772 Rosenberg et al., 2013), it is unclear, given the potential age range, as to which period
773 is represented at this point within the Jubbah basin. Elsewhere within the Nefud, ages
774 of ca. 366 and 325 ka from beneath extensive diatomite deposits (Rosenberg et al.,
775 2013) are taken to indicate lake formation during MIS 9, which was characterised by
776 undisturbed freshwater depositional conditions several metres deep. Given that the
777 thick sequence of clays dated to ca. 360 ka at Jubbah are potentially overlain by
778 deposits dated to MIS 7 (based on stratigraphic conformity at JB1 and JB2), and that
779 any interpretation of the sediments being of MIS 11 age necessitates an explanation as
780 to the conspicuous absence of MIS 9 within the Jubbah record, it is likely that
781 formation during the latter period is more plausible. During MIS 7, sedimentation
782 within the Jubbah basin was characterised by the erosion and mobilisation of slope
783 material from the adjacent sandstone outcrops. At this point the basin would have
784 exhibited a deeper profile with greater slope gradient and increased runoff potential.
785 Evidence for wetter conditions in the basin during MIS 7 is also reported by Petraglia
786 et al. (2012) (Fig. 2), and to the west of Jubbah by Rosenberg et al. (2013).

787

788 The onset of MIS 5e is marked by the existence of a large freshwater water body in
789 the basin, which likely fluctuated as a result of seasonal rainfall changes and/or
790 variations in spring discharge. The MIS 5e lake phase at Jubbah terminates with a
791 shift to shallower benthic conditions driven by reduced lake water residence times,
792 greater sensitivity to short-term P/E changes and higher evaporative losses. OSL ages
793 do not support previous estimates by Garrard et al. (1981), which suggest that lake
794 formation occurred at ca. 25 ka. It is likely that this underestimation is the result of

795 contamination by younger ^{14}C from meteoric waters (Rosenberg et al., 2013).

796 Hydroclimatic conditions during MIS 5a indicate an initial expansion of lake waters
797 within the Jubbah basin, followed by a lowering of lake levels. Palaeoecological data
798 indicate that the wider basin likely comprised a predominantly wetland environment
799 at this time, characterised by increasingly saline, brackish conditions and chemically
800 concentrated and anoxic bottom waters (e.g. Morellón et al., 2008). The record from
801 JB3 also indicates the formation of a smaller, less evaporitic, perched interdunal water
802 body during MIS 5a, which was disconnected from the main basin. An early MIS 3
803 pluvial phase from ca. 60 ka is also recorded within the Jubbah basin, and is
804 characterised by palustrine/wetland conditions with fluctuating water levels, which
805 concurs with recent finding from the Al Marrat basin ~50 km southwest of Jubbah
806 (Fig. 1) (Jennings et al., 2016). We suggest that in a similar situation to that of Al
807 Marrat, water body formation at this time was likely facilitated by recharge from the
808 Saq aquifer, during what may have been a relatively brief and weaker wet phase, in
809 comparison to those occurring during interglacials.

810

811 Palaeoecological evidence indicates the presence of a freshwater lake at the western
812 end of the basin around the Terminal Pleistocene/Holocene transition at ca. 12 ka,
813 with a high ratio of planktonic taxa, and high abundances of tychoplanktonic species
814 indicative of deeper, fresh waters. Water levels within the wider basin during the
815 Early Holocene between ca. 12 and 9 ka were astatic and evaporitic, featuring
816 predominantly eutrophic diatom species indicative of a more saline and shallow
817 wetland environment. Shallow but freshwater conditions appear to have persisted
818 across the wider basin from ca. 9 ka, with fluctuating lake levels and a predominance
819 of benthic taxa. However, the presence of freshwater mollusc species *Gyraulus*
820 *convexiusculus* at ARY, along with well-developed non-gypsiferous marls both there

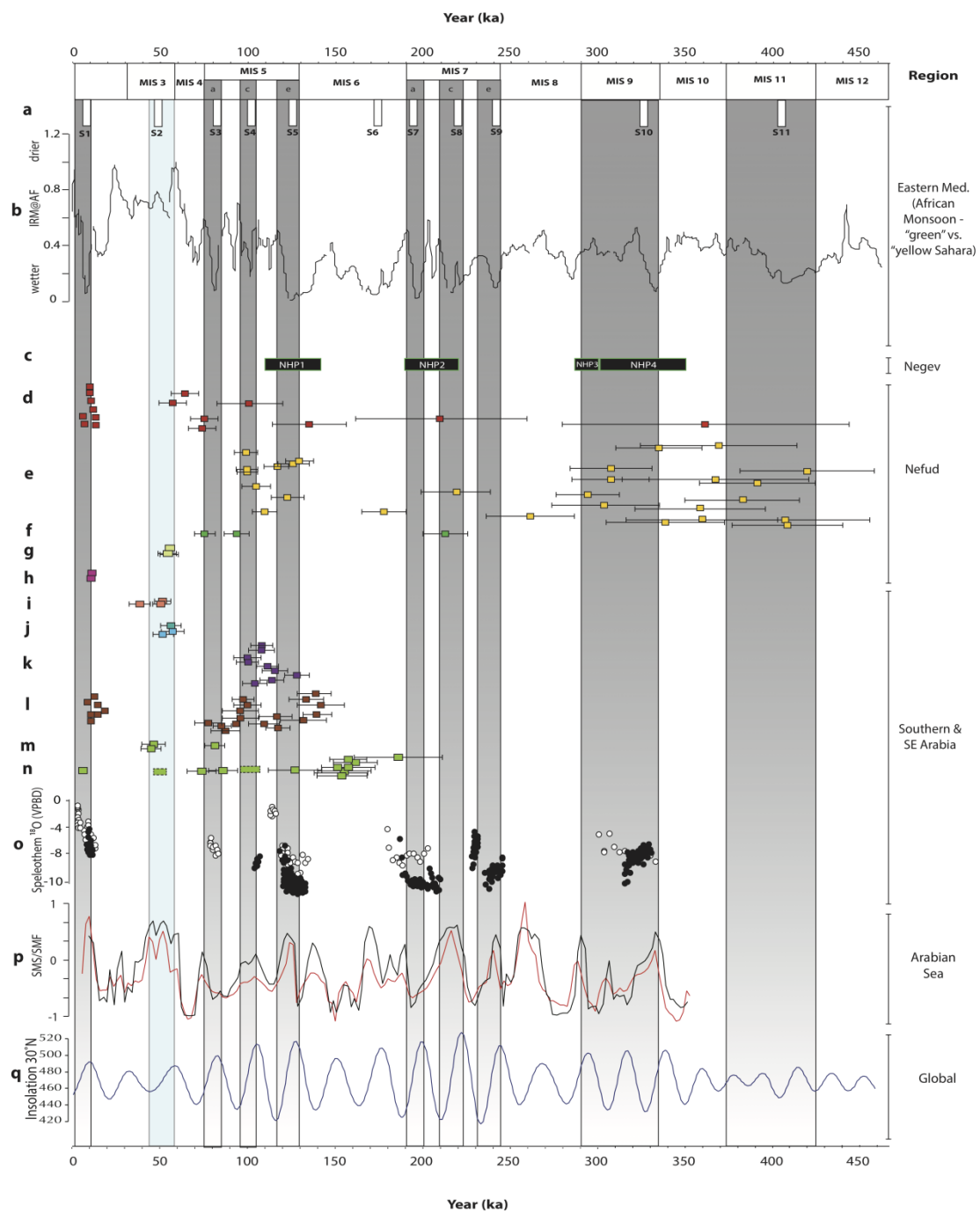
821 and at JQ101 (Crassard et al., 2013), confirm the persistence of freshwater bodies in
822 the basin until ca. 6.5 ka.

823

824 Given the longevity and apparent sensitivity of the Jubbah records it is reasonable to
825 consider the potential continuity of water body formation in the basin between pluvial
826 periods. Jubbah's history as an oasis town, and the presence of groundwater near the
827 modern surface until recent historic times, suggests that only minor rainfall increases
828 were necessary to produce standing water within the basin. Indeed,
829 palaeohydrological modelling at the Tayma oasis suggests that just 150 ± 25 mm was
830 required to initiate lake formation during the early Holocene (Engel et al., 2011). This
831 figure is similar to the current peninsula-wide average of ~ 140 mm (Almazroui et al.,
832 2013), with Jubbah itself located within 100-200 mm annual rainfall range.

833 Furthermore, in climate model simulations for 21 ka (LGM), Jubbah remains within
834 this rainfall range (Jennings et al., 2015), possibly as a result of winter storms related
835 to Mediterranean depressions and cyclogenesis west of the Zagros Mountains (Barth
836 & Steinkohl, 2004). In the absence of historic and recent intensive irrigation practices,
837 therefore, it is possible that the unique geomorphological properties of the Jubbah
838 basin would allow shallow water conditions to persist with only minimal amounts of
839 rainfall. Nonetheless, while the record from Jubbah is deep with respect to other
840 records from Arabia, sedimentation within the basin would not have been continuous
841 over the past ca. 360 ka. The Jubbah depression would have been susceptible to
842 substantial deflation during intervening arid phases, leading to hiatuses in deposition
843 between wetter periods. It is also likely that only sediments that have undergone
844 extensive diagenetic alteration and induration have been preserved, leading to the
845 preferential preservation of younger sediments, and large discontinuities present in
846 older material. As such, there is the potential for gaps to occur within those parts of
847 the sequences that represent phases of pre-Holocene rainfall increases, since much of

848 the material recording these periods may have been lost. Despite this, the
 849 correspondence of water body formation within the Jubbah basin with the wider
 850 palaeoclimatic record of Arabia provides an important means through which to assess
 851 regional climatic changes during the Mid-Late Pleistocene and Holocene periods.
 852



853

854

855 **Figure 10: Summary and comparison of key palaeoclimate records from in and**
856 **around the Arabian Peninsula. (a) Eastern Mediterranean sapropels (Zhao et al.,**
857 **2011); (b) dust flux related to wet-arid (“green” vs. “yellow” Sahara) monsoon-**
858 **driven cycles (Larrasoaña et al., 2003); (c) Negev Humid Periods derived from**
859 **speleothem records (Vaks et al., 2010); (d) Lake/wetland ages from Jubbah (this**
860 **study); (e) Nefud palaeolake ages (Rosenberg et al., 2013); (f) inferred lake age**
861 **formation at archaeological site JQ1 at Jubbah (Petraglia et al., 2012); (g)**
862 **wetland ages reported from the Nefud (Jennings et al., 2016); (h) ages of oasis**
863 **development at Tayma (Engel et al., 2011); (i) ages of fluvial channel activation**
864 **from central Saudi Arabia (McLaren et al., 2008); (j) ages from fluvio-lacustrine**
865 **sequence in eastern UAE (Parton et al., 2013); (k) ages of lake formation from**
866 **Saiwan, Oman (Rosenberg et al., 2012); (l) reported lake ages from Mundafan**
867 **and Khujaymah, southern Rub al Khali (Rosenberg et al., 2011); (m & n) ages**
868 **for the activation of the Al Ain alluvial fan system, eastern UAE, at Remah (m)**
869 **(Farrant et al., 2012) and Al Sibetah (n) (Parton et al., 2015a); (o) Speleothem**
870 **$\delta^{18}\text{O}$ records from Mukalla and Hoti Cave (summarized in Fleitmann et al.,**
871 **2011); (p) summer monsoon stack (SMS) and summer monsoon factor (SMF) of**
872 **monsoon intensity proxies from the Arabian Sea (Clemens and Prell, 2003); (q)**
873 **June insolation at 30°N (Berger and Loutre, 1991).**

874

875 *5.3. Jubbah and the wider Arabian Palaeoclimate Record*

876 Interglacial-age lake formation at Jubbah corresponds well with numerous
877 palaeoclimatic and palaeoenvironmental studies, while glacial age lake development
878 during MIS 3 supports a growing number of records attesting to a weaker wet period
879 during early MIS 3. Widespread lake/wetland development is reported from
880 elsewhere in the western Nefud during peak interglacials (e.g. Rosenberg et al., 2013;
881 Stimpson et al., 2016), in particular MIS 11, 9, 7 and 5, however, MIS 1 lake

882 formation appears to have been restricted to oases settings such as those at Jubbah
883 (Crassard et al., 2013; Hilbert et al., 2014) and Tayma (Engel et al., 2011; Ginau et
884 al., 2012). Broadly this concurs with the wider Arabian palaeoclimatic record (Fig.
885 10), which reveals an activation of hydrological systems across the peninsula during
886 eccentricity-paced interglacial maxima. In southern and southeastern regions
887 speleothem and lake records reveal an intensification and northward displacement of
888 the summer ITCZ and associated monsoon rainfall (e.g. Burns et al., 2001; Fleitmann
889 et al., 2003; 2011; Fleitmann and Matter, 2009; Matter et al., 2015; Parker et al.,
890 2004; 2006; 2016; Preston et al., 2015; Rosenberg et al., 2011; 2012;), along with the
891 widespread activation of extensive alluvial fans and drainage processes (Blechschildt
892 et al., 2009; Parton et al., 2015a; Matter et al., 2016). The phasing of terrestrial
893 rainfall increases corresponds well with marine records of summer monsoon proxies
894 from the Arabian Sea (e.g. Clemens and Prell, 2003; Des Combes et al., 2005;
895 Clemens et al., 2010), which show an abrupt decrease in dust influx, and increased
896 nutrient supply and upwelling. In the Red Sea region, an intensified EASM led to
897 freshwater influxes and lowered surface salinities (e.g. Badawi, 2014) with a
898 substantially altered wind regime across the region (Trommer et al., 2011) and high
899 summer-winter temperature ranges (e.g. Felis et al., 2004). Similarly, speleothem
900 records from the Negev reflect the strengthening of eastern Mediterranean cyclones
901 during interglacials, producing annual precipitation in excess of 300 mm (e.g. Bar-
902 Matthews et al., 2003; Vaks et al., 2010). The palaeoclimatic picture of Arabia during
903 interglacials, therefore, is one of widespread hydrological amplification featuring
904 freshwater lakes, spatially extensive perennially flowing rivers (e.g. Parton et al.,
905 2015a; Matter et al., 2016) and vegetation development.

906

907 While substantial northward displacements of the ITCZ and Indian Ocean Summer
908 Monsoon (IOSM) were the likely source of rainfall in southern and eastern regions of

909 Arabia, it is unlikely that the IOSM rainfall belt reached $\sim 27^\circ$ N (e.g. Rosenberg et
910 al., 2013; Enzel et al., 2015). While a potential contribution of rainfall from synoptic
911 conditions associated with Red Sea troughs cannot be discounted (e.g. Waldmann et
912 al., 2010), we concur with other studies (e.g. Herold and Lohmann, 2009; Jennings et
913 al., 2015; Parton et al., 2015b), which suggest that eastward zonal moisture transport
914 from an intensified East African Summer Monsoon (EASM) was likely the key
915 source of rainfall across the Nefud. Precipitation estimates of MIS 5e interglacial
916 rainfall derived from an ensemble of climate model simulations suggest that annual
917 rainfall in the region may have been up to 400 mm, with contributions from both
918 African monsoon and Westerly sources (Jennings et al., 2015). For the current
919 interglacial, numerous palaeoenvironmental archives support widespread climatic
920 amelioration. Recent COSMOS and HOL6 climate models (Guagnin et al., 2016)
921 indicate a substantial increase in rainfall at 8 ka BP, and in a similar scenario to MIS
922 5e, a northward extension of the EASM was the most likely source of rainfall.
923 Climate simulations suggest that annual precipitation during this time was highly
924 variable, ranging from lows of 20 mm to highs of 420 mm (Guagnin et al., 2016).
925

926 The environmental picture during glacials, however, is less clear. For early MIS 3, a
927 HadCM3 palaeoprecipitation model suggests that glacial-age rainfall in the region
928 may have been less than 100 mm, although the extension of the East African Summer
929 Monsoon is likely underestimated (Jennings et al., 2016). Previously it was assumed
930 that climatic conditions in Arabia during global glacial periods were too arid to
931 sustain lake development (e.g. Fleitmann et al., 2011; Rosenberg et al., 2011). While
932 marine evidence from the Arabian Sea (e.g. Clemens and Prell, 2003; Des Combes et
933 al., 2005; Caley et al., 2011a) suggests that IOSM maxima are in phase with
934 precessionally regulated summer insolation, the limited terrestrial expression of this
935 linkage has been used to suggest that precipitation and wind strength may be

936 decoupled during glacials (Fleitmann et al., 2011). A growing corpus of evidence
937 from southern and southeastern Arabia, however, now indicates that pluvial periods
938 occurred during glacials MIS 6 at ca. 160-150 ka (e.g. Wood et al., 2003; Preusser et
939 al., 2002; Parton et al., 2015) and early MIS 3 at ca. 55 ka (e.g. Krbetschek, 2008;
940 Blechschmidt et al., 2009; Farrant et al., 2012; Parton et al., 2013; 2015a; Hoffmann
941 et al., 2015). While all of these records reflect a strengthening of the glacial-age
942 IOSM, resolving the source of rainfall during MIS 3 within northwestern Arabia
943 remains problematic. African monsoon records appear to reflect increased monsoon
944 intensity during early MIS 3 (e.g. Trauth et al., 2003; Revel et al., 2010; Rohling et
945 al., 2013), synchronous with increased Nile discharge and the deposition of sapropel
946 unit S2 (Williams et al., 2015). However, the presence of this ‘debated’ sapropel
947 within the Eastern Mediterranean at ca. 55 ka may also be attributable to increased
948 stratification in the Mediterranean, as opposed to increased monsoon-fed Nile
949 discharge (see Rohling et al., 2015 for comprehensive review). In addition, evidence
950 for a wet phase at ca. 60 ka from speleothem records in Libya (Hoffmann et al.,
951 2016), suggest that the correspondence between a precessionally controlled monsoon
952 and enhanced convergence at 25-40°N as a consequence of Hadley Cell contraction,
953 may account for increased regional rainfall at this time.

954

955 As such, it remains unclear as to whether the records presented here support other
956 findings from the Nefud (Jennings et al., 2016), which suggest an intensification of
957 the EASM between ca. 55-60 ka. Further, the occurrence a precessional minimum at
958 ca. 60 ka, and an obliquity maximum at ca. 50 ka also problematize the assignment of
959 a predominant moisture source for the region during early MIS 3. Caley et al. (2011b)
960 highlight regional differences in the timing of the Indian and East African monsoons,
961 suggesting that while IOSM records contain a stronger obliquity signal, the EASM
962 responds more closely to precessional forcing. Nonetheless, while the moisture

963 source/s may remain uncertain for this period, it is likely that a strong contribution of
964 groundwater recharge, alongside small increases in precipitation, and reduced
965 evaporation, contributed to wetland development within the Nefud during early MIS
966 3.

967

968 **6. Conclusions**

969 The hydroclimatic records in the Jubbah basin comprise a unique sequence of
970 deposits that demonstrate lake/wetland formation over multiple interglacials and
971 during MIS 3. The longevity of the record at Jubbah, and the apparent sensitivity to
972 regional rainfall increases is likely a result of the basin's unique geomorphological
973 setting. Protected from the eastward transport of aeolian material, the depression has
974 not been susceptible to substantial infilling by the surrounding dunes. In addition,
975 diffuse and focussed groundwater recharge, have contributed to lake/wetland
976 formation during wet phases, with a potentially stronger groundwater influence during
977 MIS 3.

978

979 Our findings have numerous implications for understanding human demographic and
980 behavioural change. The identification of Middle Pleistocene wet periods at Jubbah
981 demonstrates windows of opportunity for hominins using Acheulian technology, and
982 by MIS 7, Middle Palaeolithic technology. The wet phases of MIS 5e, 5a and early
983 MIS 3 are associated with repeated hominin occupations of Jubbah and the
984 surrounding area (e.g. Petraglia et al., 2012; Groucutt et al., 2017; Jennings et al.,
985 2016). The significant technological differences between these assemblages are
986 consistent with their production by different populations, and probably species, of
987 hominins. The demonstration of pluvial conditions in northern Arabia in early MIS 3,
988 for instance, highlights the possibility that this area may have witnessed admixture
989 between *Homo sapiens* and Neanderthals, which is widely argued to have occurred

990 somewhere in southwest Asia ~60-50 ka (e.g. Green et al., 2010). Moving into the
991 Holocene, evidence from Jubbah demonstrates periodic lake formation between ca. 12
992 and 6 kyr BP, which thus far has not been identified in smaller depressions in the
993 dunefield (Rosenberg et al., 2013), and is likely tied to oasis development. This is in
994 keeping with growing evidence for a ‘weak connection’ between Arabia and the
995 Levant at this time, where there was some cultural diffusion from the north but
996 perhaps relatively minor population dispersal into Arabia. These findings indicate that
997 across the various wet phases of the Pleistocene and Holocene there was not a single
998 kind of human response to climate change. Rather, responses depended on the nature
999 of the environmental change and the kinds of adaptations employed by humans.
1000 Never the less, the climatic shifts identified in the Jubbah basin provide significant
1001 context to changes in human demography. Just as seeking to understand
1002 environmental conditions between peak wet periods remains a key area of research
1003 (i.e. how much water was available in places such as Jubbah between interglacials),
1004 so understanding human-environment connections in these time periods offers a key
1005 area to research. Did human populations become regionally extinct during dry
1006 phases? To what extent did oases such as Jubbah buffer populations through these
1007 phases? With increasing data available on the peak-wet phases of Arabia, such
1008 questions must animate future research in the area and allow the story of long-term
1009 interaction between humans and the environment to be told. In addition, the
1010 continually expanding palaeoclimatic picture from Arabia is one of increasing spatio-
1011 temporal heterogeneity heavily influenced by regional topographic and climatic
1012 controls, and not confined to a simplistic wet-dry dichotomy.

1013

1014

1015 **Acknowledgements**

1016 Over the last few decades the field of palaeolimnology has been significantly
1017 enhanced by the use of stable isotopes. Neil Roberts and Henry Lamb (for whom the
1018 collection of papers in this volume is dedicated) were at the forefront of this
1019 advancement amongst UK researchers, applying relatively new techniques to lakes in
1020 Africa and the Mediterranean. This study is no small way benefits from their trail
1021 blazing research. We also thank His Royal Highness Prince Sultan bin Salman,
1022 President of the Saudi Commission for Tourism and National Heritage (SCTH), and
1023 Prof. Ali Ghabban, Vice President for Antiquities and Museums, for permission to
1024 carry out this research. We thank our Saudi colleagues from the SCTH, especially
1025 Jamal Omar, Sultan Al-Fagir, and Abdulaziz al-Omari for their support and assistance
1026 with the field investigations, and two anonymous reviewers for their insightful and
1027 constructive assessments of an earlier version of the manuscript. Financial support for
1028 the fieldwork and project was provided by the European Research Council (ERC)
1029 (grant number 295719, to MDP) and the SCTH. HSG thanks the British Academy for
1030 funding.

1031

1032 **References**

1033 Al-Salamah, Ibrahim, S., Ghazaw, Y.M. and Ghumman, A.R., 2011. Groundwater
1034 modeling of Saq Aquifer Buraydah Al Qassim for better water management
1035 strategies. *Environmental monitoring and assessment*, 173(1), 851-860.

1036

1037 Almazroui, M., Abid, M. A., & Athar, H., 2013. Interannual variability of rainfall
1038 over the Arabian Peninsula using the IPCC AR4 Global Climate Models - Almazroui
1039 - 2012 - *International Journal of Climatology* - Wiley Online Library. *International*
1040 *Journal of Climatology* 33, 2328-2340.

1041

1042 Alsharhan, A.S., Rizk, Z.A., Nairn, A.E.M., Bakhit, D.W. and Alhajari, S.A. eds.,
1043 2001. Hydrogeology of an arid region: the Arabian Gulf and adjoining areas. Elsevier.
1044

1045 Auclair, M., Lamohe, M., Huot, S., 2003. Measurement of anomalous fading for
1046 feldspar IRSL using SAR. *Radiat. Meas.* 37, 487–492. doi:10.1016/S1350-
1047 4487(03)00018-0
1048

1049 Badawi, A., 2014. Late quaternary glacial/interglacial cyclicity models of the Red
1050 Sea. *Environmental Earth Sciences*. ISSN: 1866-6280 1-17. doi.org/ 10.1007/s12665-
1051 014-3446-8.
1052

1053 Bar-Matthews, M., Ayalon, A., Gilmour, M., Matthews, A., Hawkesworth, C.J., 2003.
1054 Sea- land oxygen isotope relationships from planktonic foraminifera and spe-
1055 leothems in the eastern Mediterranean region and their implication for pale- orainfall
1056 during interglacial intervals. *Geochimica et Cosmochimica Acta* 67, 3181-3199.
1057

1058 Barth, H.J., Steinkohl, F., 2004. Origin of winter precipitation in the central coastal
1059 lowland of Saudi Arabia. *Journal of Arid Environments* 5, 101-115.
1060

1061 Barthélemy, Y., Béon, O., le Nindre, Y.M., Munaf, S., Poitrinal, D., Gutierrez, A.,
1062 Vandenbeusch, M., Al Shoaibi, A. and Wijnen, M., 2007. Modelling of the Saq
1063 aquifer system (Saudi Arabia). *Aquifer Systems Management: Darcy's Legacy in a*
1064 *World of Impending Water Shortage*. Taylor & Francis, London, pp.175-190.
1065

1066 Battarbee, R., 2000. Palaeolimnological approaches to climate change, with special
1067 regard to the biological record. *Quaternary Science Reviews*, 19(1-5), 107–124.
1068

1069 Battarbee, R. W., Jones, V. J., Flower, R. J., Cameron, N. G., Bennion, H., Carvalho,
1070 L. and Juggins, S., 2001. Diatoms. In: J. P. Smol, Birks, H. J. B. and Last, W. M.
1071 (eds) Tracking Environmental Change Using Lake Sediments, Volume 3: Terrestrial,
1072 Algal and Siliceous Indicators. Dordrecht, The Netherlands, Kluwer Academic
1073 Publishers. 155-202.
1074
1075 Bennett, K.D. (1996) Determination of the Number of Zones in a Biostratigraphical
1076 Sequence. *New Phytologist*, 132(1), 155-170.
1077
1078 Berger, A., Loutre, M.F., 1991. Insolation values for the climate of the last 10 million
1079 years. *Quaternary Science Reviews* 10 (4), 297-317.
1080
1081 Blechschmidt, I., Matter, A., Preusser, F., Rieke-Zapp, D., 2009. Monsoon triggered
1082 formation of Quaternary alluvial megafans in the interior of Oman. *Geomorphology*
1083 110, 128-139.
1084
1085 Blunt, L.A., 1881. *A Pilgrimage to Nejd: The Cradle of the Arab Race* (Vol. 1). J.
1086 Murray.
1087
1088 Bramkamp, R.A., Brown, G.F., Holm, D.A. and Layne Jr, N.M., 1963. Geologic map
1089 of the Wadi as Sirhan quadrangle, Kingdom of Saudi Arabia (No. 200-A). US
1090 Geological Survey.
1091
1092 Breeze, P., N. A. Drake, R. G. Jennings, A. Parton, H. S. Groucutt, L. Clark-Balzan,
1093 C. Shipton, T. White, M. D. Petraglia, and A. Alsharekh. 2015. Remote Sensing and
1094 GIS Techniques for Reconstructing Arabian Paleohydrology and Identifying
1095 Archaeological Sites. *Quaternary International* 382, 98–119.

1096

1097 Bronk Ramsey, C., Higham, T.F.G., Owen, D.C., Pike, A.W.G., Hedges, R.E.M.,
1098 2002. Radiocarbon dates from the Oxford AMS system: Archaeometry Datelist 31.
1099 Archaeometry 44, 1–149.

1100

1101 Bronk Ramsey, C., Higham, T., Leach, P., 2004. Towards high-precision AMS:
1102 Progress and limitations. Radiocarbon 46, 17–24.

1103

1104 Bronk Ramsey, C., 2009. Bayesian analysis of radiocarbon dates. Radiocarbon 51,
1105 337–360.

1106

1107 Burns, S.J., Fleitmann, D., Matter, A., Neff, U., Mangini, A., 2001. Speleothem
1108 evidence from Oman for continental pluvial events during interglacial periods.
1109 Geology 29 (7), 623–626.

1110

1111 Caley, T., Malaize, B., Zaragossi, S., Rossignol, L., Bourget, J., Eynaud, F., Martinez,
1112 P., Giraudeau, J., Charlier, K., Ellouz-Zimmermann, N., 2011a. New Arabian Sea
1113 records help decipher orbital timing of Indo-Asian monsoon. Earth and Plan-
1114 etary Science Letters 308 (3e4), 433-444.

1115

1116 Caley, T., Malaize, B., Revel, M., Ducassou, E., Wainer, K., Ibrahim, M., Shoeaib,
1117 D., Mi-geon, M., Marieu, V., 2011b. Orbital timing of the Indian, East Asian and
1118 African boreal monsoons and the concept of a “global monsoon”. Quaternary Science
1119 Reviews 30, 3705-3715.

1120

1121 Clark-Balzan, L., 2016. Source and characteristics of blue , infrared (IR), and post-IR
1122 IR stimulated signals from gypsum-rich samples. Anc. TL 34, 6–13.

1123

1124 Clark-Balzan, L., Parton, A., Breeze, P.S., Groucutt, H.S. and Petraglia, M.D., 2017.

1125 Resolving problematic luminescence chronologies for carbonate-and evaporite-rich

1126 sediments spanning multiple humid periods in the Jubbah basin, Saudi

1127 Arabia. *Quaternary Geochronology*, *in press*, doi: 10.1016/j.quageo.2017.06.002.

1128

1129 Clemens, S., Prell, W.L., 2003. A 350,000 year summer-monsoon multi-proxy stack

1130 from the Owen Ridge, Northern Arabian Sea. *Marine Geology* 201, 35-51.

1131

1132 Clemens, S.C., Prell, W.L., Sun, Y., 2010. Orbital-scale timing and mechanisms

1133 driving Late Pleistocene Indo-Asian summer monsoons: reinterpreting cave speleo-

1134 them d18O. *Paleoceanography* 25, PA4207. doi.org/10.1029/2010PA001926. □

1135

1136 Crassard, R., Petraglia, M.D., Parker, A.G., Parton, A., Roberts, R.G., Jacobs, Z.,

1137 Alsharekh, A., Al-Omari, A., Breeze, P., Drake, N.A., Groucutt, H.S., Jennings, R.,

1138 Régagnon, E., Shipton, C., 2013. Beyond the Levant: first evidence of a pre-pottery

1139 Neolithic incursion into the Nefud Desert, Saudi Arabia. *PLoS ONE* 8 (7), e68061.

1140

1141 Dean Jr, W.E., 1974. Determination of carbonate and organic matter in calcareous

1142 sediments and sedimentary rocks by loss on ignition: comparison with other

1143 methods. *Journal of Sedimentary Research*, 44(1).

1144

1145 Dearing, J., 1999. Magnetic susceptibility. *Environmental magnetism: A practical*

1146 *guide*, 6, pp.35-62.

1147

1148 Des Combes, H.J., Caulet, J.P., Tribovillard, N., 2005. Monitoring the variations of
1149 the Socotra upwelling system during the last 250 kyr: a biogenic and geochemical
1150 approach. *Palaeogeography, Palaeoclimatology, Palaeoecology* 223, 243-259.
1151

1152 Dill, H.G., 2011. A comparative study of uranium – thorium accumulation at the
1153 western edge of the Arabian Peninsula and mineral deposits worldwide. *Arab. J.*
1154 *Geosci.* 4, 123–146. doi:10.1007/s12517-009-0107-4
1155

1156 Dincer, T., Al-Mugrin, A., & Zimmermann, U., 1974. Study of the infiltration and
1157 recharge through the sand dunes in arid zones with special reference to the stable
1158 isotopes and thermonuclear tritium. *Journal of Hydrology*, 23, 79-109.
1159

1160 Duller, G.A.T., 2003. Distinguishing quartz and feldspar in single grain luminescence
1161 measurements. *Radiat. Meas.* 37, 161–165. doi:10.1016/S1350-4487(02)00170-1
1162

1163 Durcan, J.A., King, G.E., Duller, G.A. T., 2015. DRAC: Dose Rate and Age
1164 Calculator for trapped charge dating. *Quat. Geochronol.* 28, 54–61.
1165 doi:10.1016/j.quageo.2015.03.012
1166

1167 Engel, M., Brückner, H., Pint, A., Wellbrock, K., Ginau, A., Voss, P., Grottker, M.,
1168 Klasen, N., Frenzel, P., 2011. The early Holocene humid period in NW Saudi Arabia
1169 – Sediments, microfossils and palaeo-hydrological modelling. *Quaternary*
1170 *International.* doi.org/10.1016/j.quaint.2011.04.028
1171

1172 Farrant, A.R., Ellison, R.A., Thomas, R.J., Pharaoh, T.C., Newell, A.J., Goodenough,
1173 K.M., Lee, J.R., Knox, R.O., 2012. The geology and geophysics of the United Arab

1174 Emirates. In: *Geology of the Western and Central United Arab Emirates*. British
1175 Geological Survey, vol. 6. Keyworth, Nottingham, p. 371.
1176
1177 Faure, G., 1986. *Principles of Isotope Geology* (2nd ed.). John Wiley & Sons, New
1178 York.
1179
1180 Felis, T., Lohmann, G., Kuhnert, H., Lorenz, S.J., Scholz, D., Patzold, J., Al-Rousan,
1181 S.A., Al-Moghrabi, S.M., 2004. Increased seasonality in Middle East temperatures
1182 during the Last Interglacial period. *Nature* 429, 164-168.
1183
1184 Fisk, E.P. and Pim, R.H., 1985. *Hydrogeological appraisal* (August 1983 to May
1185 1985). Rep. Tabuk Agric. Dev. Co., Tabuk, 58 pp.
1186
1187 Fleitmann, D., Burns, S.J., Neff, U., Mangini, A., Matter, A., 2003. Changing
1188 moisture sources over the last 330,000 years in Northern Oman from fluid-inclusion
1189 evidence in speleothems. *Quaternary Research* 60, 223-232. □
1190
1191 Fleitmann, D., Matter, A. 2009. The speleothem record of climate variability in
1192 Southern Arabia. *Geoscience* 341: 633–642.
1193
1194 Fleitmann, D., Burns, S.J., Pekala, M., Mangini, A., Al-Subbary, A., Al-Aowah, M.,
1195 Kramers, J., Matter, A., 2011. Holocene and Pleistocene pluvial periods in Yemen,
1196 southern Arabia. *Quaternary Science Reviews* 30, 783-787.
1197
1198 Garrard, A.N., Harvey, C.P.D., Switsur, V.R., 1981. Environment and settlement
1199 during the Upper Pleistocene and Holocene at Jubba in the Great Nefud, northern
1200 Arabia. *ATLAL - Journal of Saudi Arabian Archaeology* 5, 137-148.

1201

1202 Garzanti, E., Vermeesch, P., Andò, S., Vezzoli, G., Valagussa, M., Allen, K., Kadi,
1203 K.A., Al-Juboury, A.I.A., 2013. Provenance and recycling of Arabian desert sand.
1204 *Earth-Science Rev.* 120, 1–19. doi:10.1016/j.earscirev.2013.01.005

1205

1206 Ginau, A., Engel, M., & Brückner, H., 2012. Holocene chemical precipitates in the
1207 continental sabkha of Tayma (NW Saudi Arabia). *Journal of Arid Environments* 84,
1208 26-37.

1209

1210 Green, R.E., Krause, J., Briggs, A.W., Maricic, T., Stenzel, U., Kircher, M., Patterson,
1211 N., Li, H., Zhai, W., Fritz, M.H.Y. and Hansen, N.F., 2010. A draft sequence of the
1212 Neandertal genome. *Science*, 328(5979), 710-722.

1213

1214 Groucutt, H. S., Petraglia, M. D., Bailey, G., Scerri, E. M. L., Parton, A., Clark-
1215 Balzan, L., Jennings, R. P., Lewis, L., Blinkhorn, J., Drake, N. A., Breeze, P. S.,
1216 Inglis, R. H., Devès, M. H., Meredith-Williams, M., Boivin, N., Thomas, M. G.,
1217 Scally, A. 2015a. Rethinking the dispersal of *Homo sapiens* out of Africa.
1218 *Evolutionary Anthropology: Issues, News, and Reviews*, 24(4), 149–164.
1219 <http://doi.org/10.1002/evan.21455>

1220

1221 Groucutt, H.S., White, T.S., Clark-Balzan, L., Parton, A., Crassard, R., Shipton, C.,
1222 Jennings, R.P., Parker, A.G., Breeze, P.S., Scerri, E.M.L., Alsharekh, A., Petraglia,
1223 M.D., 2015b. Human occupation of the Arabian Empty Quarter during MIS 5:
1224 Evidence from Mundafan Al-Buhayrah, Saudi Arabia. *Quaternary Science Reviews*.
1225 119, 116–135. doi:10.1016/j.quascirev.2015.04.020

1226

1227 Groucutt, H. S., E. M. L. Scerri., L. Lewis, L. Clark-Balzan, J. Blinkhorn, R. P.
1228 Jennings, A. Parton, and M. D. Petraglia. 2015c. Stone tool assemblages and models
1229 for the dispersal of *Homo sapiens* out of Africa. *Quaternary International* 382, 8–30.
1230 doi.org/10.1016/j.quaint.2015.01.039
1231
1232 Groucutt, H. S., Scerri, E. M. L., Amor, K., Shipton, C., Jennings, R. P., Parton, A.,
1233 Clark-Balzan, L., Alsharekh, A., Petraglia, M. D., 2017. Middle Palaeolithic raw
1234 material procurement and early stage reduction at Jubbah, Saudi Arabia.
1235 *Archaeological Research in Asia*, 9, 44–62. doi.org/10.1016/j.ara.2017.01.003
1236
1237 Grove, M., 2012. Amplitudes of orbitally induced climatic cycles and patterns of
1238 hominin speciation. *Journal of Archaeological Science*, 39(10), 3085–3094.
1239 doi.org/10.1016/j.jas.2012.04.023
1240
1241 Guagnin, M., Jennings, R.P., Clark-Balzan, L., Groucutt, H.S., Parton, A. and
1242 Petraglia, M.D., 2015. Hunters and herders: Exploring the Neolithic transition in the
1243 rock art of Shuwaymis, Saudi Arabia. *Archaeological Research in Asia*, 4, 3-16.
1244
1245 Guagnin, M., Jennings, R., Eager, H., Parton, A., Stimpson, C., Stepanek, C., Pfeiffer,
1246 M., Groucutt, H.S., Drake, N.A., Alsharekh, A. and Petraglia, M.D., 2016. Rock art
1247 imagery as a proxy for Holocene environmental change: A view from Shuwaymis,
1248 NW Saudi Arabia. *The Holocene*, 26(11), 1822-1834.
1249
1250 Guérin, G., Mercier, N., Adamiec, G., 2011. Dose-rate conversion factors: Update.
1251 *Anc. TL* 29, 5–8.
1252

1253 Hamilton, P., 2010. *Brachysira brebissonii*. In: Diatoms of the United States.
1254 http://westerndiatoms.colorado.edu/taxa/species/brachysira_brebissonii
1255

1256 Heiri, O., Lotter, A.F. and Lemcke, G., 2001. Loss on ignition as a method for
1257 estimating organic and carbonate content in sediments: reproducibility and
1258 comparability of results. *Journal of paleolimnology*, 25(1), 101-110.
1259

1260 Herold, M., Lohmann, G., 2009. Eemian tropical and subtropical African moisture
1261 transport: an isotope modelling study. *Climate Dynamics* 33, 1075-1088.
1262

1263 Hilbert, Y.H., White, T.S., Parton, A., Clark-Balzan, L., Crassard, R., Groucutt, H.S.,
1264 Jennings, R.P., Breeze, P., Parker, A., Shipton, C., Al-Omari, A., Alsharekh, A.M.,
1265 Petraglia, M.D., 2014. Epipalaeolithic occupation and palaeoenvironments of the
1266 southern Nefud desert, Saudi Arabia, during the Terminal Pleistocene and Early
1267 Holocene. *J. Archaeol. Sci.* 50, 460–474. doi:10.1016/j.jas.2014.07.023
1268

1269 Hoffmann, G., Rupprechter, M., & Rahn, M., Preusser, F., 2015. Fluvio-lacustrine
1270 deposits reveal precipitation pattern in SE Arabia during early MIS 3. *Quaternary*
1271 *International* 382, 145-153
1272

1273 Huntley, D.J., Lamothe, M., 2001. Ubiquity of anomalous fading in K-feldspars and
1274 the measurement and correction for it in optical dating. *Can. J. Earth Sci.* 38, 1093–
1275 1106. doi:10.1139/e01-013
1276

1277 Hussein, M.T., Bazuhair, A.G. and Ageeb, A.E., 1992. Hydrogeology of the Saq
1278 formation east of Hail, northern Saudi Arabia. *Quarterly Journal of Engineering*
1279 *Geology and Hydrogeology*, 25(1), 57-64.

1280

1281 Jennings, R., Parton, A., Groucutt, H., Clark-Balzan, L., Breeze, P., Drake, N. A.,
1282 Alsharekh, A., Petraglia, M. D. 2014. High-resolution geospatial surveying
1283 techniques provide new insights into rock-art landscapes at Shuwaymis, Saudi Arabia.
1284 *Arabian Archaeology and Epigraphy*, 25, 1–21.

1285

1286 Jennings, R.P., Singarayer, J., Stone, E.J., Krebs-Kanzow, U., Khon, V., Nisancioglu,
1287 K.H., Pfeiffer, M., Zhang, X., Parker, A., Parton, A., Groucutt, H.S., White, T.S.,
1288 Drake, N.A., Petraglia, M.D., 2015. The greening of Arabia: multiple opportunities
1289 for human occupation of the Arabian Peninsula during the Late Pleistocene inferred
1290 from an ensemble of climate model simulations. *Quat. Int.* 382, 181-199.
1291 doi.org/10.1016/j.quaint.2015.01.006.

1292

1293 Jennings, R. P., Parton, A., Clark-Balzan, L., White, T. S., Groucutt, H. S., Breeze, P.
1294 S., Parker, A. G., Drake, N. A., Petraglia, M. D., 2016. Human occupation of the
1295 northern Arabian interior during early Marine Isotope Stage 3. *Journal of Quaternary*
1296 *Science*, 31(8), 953–966. doi.org/10.1002/jqs.2920

1297

1298 Kaufman, A., Ghaleb, B., Wehmiller, J.F., Hillaire-Marcel, C., 1996. Uranium
1299 concentration and isotope ratio profiles within *Mercenaria* shells: Geochronological
1300 implications. *Geochim. Cosmochim. Acta* 60, 3735–3746. [doi:10.1016/0016-](https://doi.org/10.1016/0016-7037(96)00190-1)
1301 [7037\(96\)00190-1](https://doi.org/10.1016/0016-7037(96)00190-1)

1302

1303 Krammer, K. and Lange-Bertalot, H., 1986. *Bacillariophyceae* 1. Teil *Naviculaceae*.
1304 Stuttgart, Gustav Fisher Verlag.

1305

- 1306 Krammer, K. and Lange-Bertalot, H., 1988. Bacillariophyceae 2. Teil Epithemiaceae,
1307 Surirellaceae. Stuttgart, Gustav Fisher Verlag
1308
- 1309 Krammer, K. and Lange-Bertalot, H., 1991a. Bacillariophyceae 3. Teil Centrales,
1310 Fragilariaceae, Eunotiaceae. Stuttgart, Gustav Fisher Verlag
1311
- 1312 Krammer, K. and Lange-Bertalot, H., 1991b. Bacillariophyceae 4. Teil
1313 Achnanthaceae, Kritische Ergänzungen zu Navicula (Lineolate) und Gomphonema.
1314 Stuttgart, Gustav Fisher Verlag
1315
- 1316 Krbetschek, M.R., Rieser, U., Zöller, L., Heinicke, J., 1994. Radioactive disequilibria
1317 in palaeodosimetric dating of sediments. Radiat. Meas. 23, 485–489.
1318
- 1319 Lamb, A.L., Leng, M.J., Lamb, H.F., Mohammed, M.U., 2000. A 9000-year oxygen
1320 and carbon isotope record of hydrological change in a small Ethiopian crater lake.
1321 The Holocene 10, 167-177.
1322
- 1323 Larrasoaña, J. C., Roberts, A. P., Rohling, E. J., Winklhofer, M., and Wehausen, R.
1324 (2003). Three million years of monsoon variability over the northern Sahara. Climate
1325 Dynamics 21, 689–698.
1326
- 1327 Legezynska, E., Wiktor, K., 1981. Bottom fauna of the Inner Puck Bay. Zesz. Nauk.
1328 UG, Oceanografia, 8, 63-77.
1329
- 1330 Leng, M.J. and Marshall, J.D., 2004. Palaeoclimate interpretation of stable isotope
1331 data from lake sediment archives. Quaternary Science Reviews, 23(7), 811-831.
1332

1333 Lloyd, J.W. and Pim, R.H., 1990. The hydrogeology and groundwater resources
1334 development of the Cambro-Ordovician sandstone aquifer in Saudi Arabia and
1335 Jordan. *Journal of Hydrology*, 121(1-4), 1-20.
1336
1337 Marty, J., Myrbo, A., 2014. Radiocarbon dating suitability of aquatic plant
1338 macrofossils. *J. Paleolimnol.* 52: 435-443. doi:10.1007/s10933-014-9796-0
1339
1340 Maslin, M. A., Brierley, C. M., Milner, A. M., Shultz, S., Trauth, M. H., Wilson, K.
1341 E. 2014. East African climate pulses and early human evolution. *Quaternary Science*
1342 *Reviews.* 301, 1-17. doi.org/10.1016/j.quascirev.2014.06.012 □
1343
1344 Matter, A., Neubert, E., Preusser, F., Rosenberg, T., Al-Wagdani, K., 2015. Palaeo-
1345 environmental implications derived from lake and sabkha deposits of the southern
1346 Rub' al-Khali, Saudi Arabia and Oman. *Quat. Int.* 382, 120–131.
1347
1348 Matter, A., Mahjoub, A., Neubert, E., Preusser, F., Schwalb, A., Szidat, S., Wulf, G.,
1349 2016. Reactivation of the Pleistocene trans-Arabian Wadi ad Dawasir fluvial system
1350 (Saudi Arabia) during the Holocene humid phase. *Geomorphology* 270, 88–101.
1351
1352 McClure, H.A., 1976. Radiocarbon chronology of late Quaternary lakes in the
1353 Arabian desert. *Nature* 263, 755.
1354
1355 Meyers, D., 2014. *Epithemia argus*. In: *Diatoms of the United States*.
1356 http://westerndiatoms.colorado.edu/taxa/species/epithemia_argus
1357
1358 Morellón, M., Valero-Garcés, B., Moreno, A., González-Sampériz, P., Mata, P.,
1359 Romero, O., Maestro, M. and Navas, A., 2008. Holocene palaeohydrology and

1360 climate variability in northeastern Spain: the sedimentary record of Lake Estanya
1361 (Pre-Pyrenean range). *Quaternary International*, 181(1), 15-31.
1362
1363 Murray, A.S., Wintle, A.G., 2000. Luminescence dating of quartz using an improved
1364 single-aliquot regenerative-dose protocol. *Radiat. Meas.* 32, 57–73.
1365 doi:10.1016/S1350-4487(99)00253-X
1366
1367 Murray, A.S., Wintle, A.G., 2003. The single aliquot regenerative dose protocol:
1368 Potential for improvements in reliability. *Radiat. Meas.* 37, 377–381.
1369 doi:10.1016/S1350-4487(03)00053-2
1370
1371 Nakov, T., Guillory, W., Julius, M., Theriot, E. and Alverson, A., 2015. Towards a
1372 phylogenetic classification of species belonging to the diatom genus *Cyclotella*
1373 (*Bacillariophyceae*): Transfer of species formerly placed in *Puncticulata*,
1374 *Handmannia*, *Pliocaenicus* and *Cyclotella* to the genus *Lindavia*. *Phytotaxa*, 217(3),
1375 249-264.
1376
1377 Nathan, R.P., Mauz, B., 2008. On the dose-rate estimate of carbonate-rich sediments
1378 for trapped charge dating. *Radiat. Meas.* 43, 14–25.
1379 doi:10.1016/j.radmeas.2007.12.012
1380
1381 Nathan, R.P., Thomas, P.J., Jain, M., Murray, a. S., Rhodes, E.J., 2003.
1382 Environmental dose rate heterogeneity of beta radiation and its implications for
1383 luminescence dating: Monte Carlo modelling and experimental validation. *Radiat.*
1384 *Meas.* 37, 305–313. doi:10.1016/S1350-4487(03)00008-8
1385

1386 Olley, J.M., Murray, A., Roberts, R.G., 1996. The effects of disequilibria in the
1387 uranium and thorium decay chains on burial dose rates in fluvial sediments. *Quat. Sci.*
1388 *Rev.* 15, 751-760.

1389

1390 Oswald, W.W., Anderson, P.M., Brown, T.A., Brubaker, L.B., Hu, F.S., Lozhkin, A.
1391 V, Tinner, W., Kaltenrieder, P., 2005. Effects of sample mass and macrofossil type on
1392 radiocarbon dating of arctic and boreal lake sediments. *The Holocene* 15, 758–767.

1393

1394 Parker, A.G., Eckersley, L., Smith, M.M., Goudie, A.S., Stokes, S., White, K.,
1395 Hodson, M.J., 2004. Holocene vegetation dynamics in the northeastern Rub' al-Khali
1396 desert, Arabian Peninsula: a pollen, phytolith and carbon isotope study. *Journal of*
1397 *Quaternary Science* 19, 665–676.

1398

1399 Parker, A.G., Goudie, A.S., Stokes, S., White, K., Hodson, M.J., Manning, M.,
1400 Kennet, D., 2006. A record of Holocene climate change from lake geochemical
1401 analyses in south-eastern Arabia. *Quat. Res.* 66, 465–476.

1402

1403 Parker, A. G., Preston, G. W., Parton, A., Walkington, H., Jardine, P. E., Leng, M. J.,
1404 & Hodson, M. J., 2016. Low-latitude Holocene hydroclimate derived from lake
1405 sediment flux and geochemistry. *Journal of Quaternary Science*, 31(4), 286–299.
1406 doi.org/10.1002/jqs.2859

1407

1408 Parton, A., Farrant, A.R., Leng, M.J., Schwenninger, J.-L., Rose, J.I., Uerpmann, H.-
1409 P., Parker, A.G., 2013. An early MIS 3 pluvial phase in Southeast Arabia: climatic
1410 and archaeological implications. *Quaternary International* 300, 62-74.

1411

1412 Parton, A., Farrant, A.R., Lang, M.J., Telfer, M.W., Groucutt, H.S., Petraglia, M.D.,
1413 Parker, A.G., 2015a. Alluvial fan records from southeast Arabia reveal multiple
1414 windows for human dispersal. *Geology* 43 (4), 295-298. doi.org/ 10.1130/g36401.1.
1415
1416 Parton, A., White, T.S., Parker, A., Breeze, P.S., Jennings, R., Groucutt, H.S.,
1417 Petraglia, M.D., 2015b. Orbital-scale climate variability in Arabia as a potential motor
1418 for human dispersals. *Quat. Int.* 382, 82e97. doi.org/10.1016/ j.quaint.2015.01.005.
1419
1420 Petraglia, M.D., Alsharekh, A.M., Crassard, R., Drake, N.A., Groucutt, H., Parker,
1421 A.G., Roberts, R.G., 2011. Middle Paleolithic occupation on a Marine Isotope Stage 5
1422 lakeshore in the Nafud Desert, Saudi Arabia. *Quaternary Science Reviews* 30, 1555-
1423 1559.
1424
1425 Petraglia, M.D., Alsharekh, A., Breeze, P., Clarkson, C., Crassard, R., Drake, N.A.,
1426 Groucutt, H.S., Jennings, R., Parker, A.G., Parton, A., Roberts, R.G., Shipton, C.,
1427 Matheson, C., al-Omari, A., Veall, M. A., 2012. Hominin dispersal into the Nefud
1428 desert and Middle Palaeolithic settlement along the Jubbah palaeolake, northern
1429 Arabia. *PLoS ONE* 7, e49840.
1430
1431 Poulíčková, A. and Jahn, R., 2007. *Campylodiscus clypeus* (Ehrenberg) Ehrenberg ex
1432 Kützing: Typification, morphology and distribution. *Diatom Research*, 22(1), 135-
1433 146.
1434
1435 Preston, G.W., Thomas, D.S.G., Goudie, A.S., Atkinson, O.A.C., Leng, M.J., Hodson,
1436 M.J., Walkington, H., Charpentier, V., Méry, S., Borgi, F., Parker, A.G., 2015. A
1437 multi-proxy analysis of the Holocene humid phase from the United Arab Emirates

1438 and its implications for southeast Arabia's Neolithic populations. *Quat. Int.* 382, 277–
1439 292.

1440

1441 Preusser, F., Radies, D., Matter, A., 2002. A 160,000 year record of dune
1442 development and atmospheric circulation in Southern Arabia. *Science* 296, 2018-2020.

1443

1444 Radies, D., Hasiotis, S.T., Preusser, F., Neubert, E., Matter, A., 2005. Paleoclimatic
1445 significance of Early Holocene faunal assemblages in wet interdune deposits of the
1446 Wahiba Sand Sea, Sultanate of Oman. *J. Arid Environ.* 62, 109–125.

1447

1448 Reimer, P.J., Bard, E., Bayliss, A., Beck, J.W., Blackwell, P.G., Bronk Ramsey, C.,
1449 Buck, C.E., Cheng, H., Edwards, R.L., Friedrich, M., Grootes, P.M., Guilderson, T.P.,
1450 Hafliðason, H., Hajdas, I., Hatté, C., Heaton, T.J., Hoffmann, D.L., Hogg, A.G.,
1451 Hughen, K.A., Kaiser, K.F., Kromer, B., Manning, S.W., Niu, M., Reimer, R.W.,
1452 Richards, D.A., Scott, E.M., Southon, J.R., Staff, R.A., Turney, C.S.M., van der
1453 Plicht, J., 2013. IntCal13 and Marine13 Radiocarbon Age Calibration Curves 0-
1454 50,000 Years cal BP. *Radiocarbon* 55, 1869–1887. doi:10.2458/azu_js_rc.55.16947

1455

1456 Renberg, I., 1990. A procedure for preparing large sets of diatom slides from
1457 sediment cores. *Journal of Paleolimnology*, 4(1), 87-90.

1458

1459 Revel, M.E., Ducassou, E., Grousset, F.E., Bernasconi, S.M., Migeon, S., Revillon,
1460 S., Mascle, J., Murat, A., Zaragosi, S., Bosch, D., 2010. 100,000 years of African
1461 monsoon variability recorded in sediments of the Nile margin. *Quaternary Science*
1462 *Reviews* 29, 1342–1362

1463

1464 Rosenberg, T.M., Preusser, F., Fleitmann, D., Schwalb, A., Penkman, K., Schmid,
1465 T.W., Al-Shanti, M.A., Kadi, K., Matter, A., 2011a. Humid periods in southern
1466 Arabia: Windows of opportunity for modern human dispersal. *Geology* 39, 1115–
1467 1118. doi:10.1130/G32281.1
1468
1469 Rosenberg, T.M., Preusser, F., Wintle, A.G., 2011b. A comparison of single and
1470 multiple aliquot TT-OSL data sets for sand-sized quartz from the Arabian Peninsula.
1471 *Radiat. Meas.* 46, 573–579. doi:10.1016/j.radmeas.2011.03.020
1472
1473 Rosenberg, T.M., Preusser, F., Risberg, J., Plikk, A., Kadi, K.K., Matter, A.,
1474 Fleitmann, D., 2013. Middle and Late Pleistocene humid periods recorded in
1475 palaeolake deposits of the Nafud desert, Saudi Arabia. *Quaternary Science Reviews*
1476 70, 109-123. □
1477
1478 Saros, J. E. and Anderson, N. J., 2014. The ecology of the planktonic diatom
1479 *Cyclotella* and its implications for global environmental change studies. *Biological*
1480 *Reviews*. doi: 10.1111/brv.12120
1481
1482 Scerri, E. M. L., S. P. Breeze, A. Parton, H. S. Groucutt, T. S. White, C. Stimpson, L.
1483 Clark-Balzan, R. Jennings, A. Alsharekh, and M. D. Petraglia. 2015. Middle to Late
1484 Pleistocene Human Habitation in the Western Nefud Desert, Saudi Arabia.
1485 *Quaternary International* 382, 200–214.
1486
1487 Shea, J. J., 2008. Transitions or turnovers? Climatically-forced extinctions of *Homo*
1488 *sapiens* and Neanderthals in the east Mediterranean Levant. *Quaternary Science*
1489 *Reviews*, 27(23-24), 2253–2270. doi.org/doi:10.1016/j.quascirev.2008.08.015
1490

1491 Shipton, C., Parton, A., Breeze, P., Jennings, R., Groucutt, H.S., White, T.S., Drake,
1492 N., Crassard, R., Alsharekh, A., Petraglia, M.D., 2014. Large Flake Acheulean in the
1493 Nefud Desert of northern Arabia. *Paleoanthropology* 2014, 446-462.

1494

1495 Spaulding, S., and Metzeltin, D., 2011. *Rhopalodia*. In *Diatoms of the United States*.
1496 <http://westerndiatoms.colorado.edu/taxa/genus/rhopalodia>

1497

1498 Staubwasser, M., & Weiss, H., 2006. Holocene climate and cultural evolution in late
1499 prehistoric–early historic West Asia. *Quaternary Research*, 66(3), 372–387.

1500

1501 Stimpson, C.M., Lister, A., Parton, A., Clark-Balzan, L., Breeze, P.S., Drake, N.A.,
1502 Groucutt, H.S., Jennings, R., Scerri, E.M., White, T.S., Zahir, M., 2016. Middle
1503 Pleistocene vertebrate fossils from the Nefud Desert, Saudi Arabia: implications for
1504 biogeography and palaeoecology. *Quaternary Science Reviews*, 143, 13-36.

1505

1506 Ter Braak, C.J. and Prentice, I.C., 1988. A theory of gradient analysis. *Advances in*
1507 *ecological research*, 18, 271-317.

1508

1509 Thatcher, L., Rubin, M., Brown, G.F., 1961. Dating Desert Ground Water. *Science*
1510 (3472). 134, 105–106.

1511

1512 Thiel, C., Buylaert, J.P., Murray, A., Terhorst, B., Hofer, I., Tsukamoto, S., Frechen,
1513 M., 2011a. Luminescence dating of the Stratzing loess profile (Austria)—Testing the
1514 potential of an elevated temperature post-IR IRSL protocol. *Quat. Int.* 234, 23–31.
1515 doi:10.1016/j.quaint.2010.05.018

1516

1517 Thiel, C., Buylaert, J.-P., Murray, A.S., Tsukamoto, S., 2011b. On the applicability of
1518 post-IR IRSL dating to Japanese loess. *Geochronometria* 38, 369–378.
1519 doi:10.2478/s13386-011-0043-4
1520

1521 Trauth, M. H., Deino, A. L., Bergner, A. G. N., & Strecker, M. R., 2003. East African
1522 climate change and orbital forcing during the last 175 kyr BP. *Earth and Planetary
1523 Science Letters*, 206(3-4), 297–313. doi.org/10.1016/S0012-821X(02)01105-6
1524

1525 Trauth, M. H., Maslin, M. A., Deino, A. L., Strecker, M. R., Bergner, A. G. N., &
1526 Dühnforth, M., 2007. High- and low-latitude forcing of Plio-Pleistocene East African
1527 climate and human evolution. *Journal of Human Evolution*, 53(5), 475–486.
1528 doi.org/10.1016/j.jhevol.2006.12.009
1529

1530 Trommer, G., Siccha, M., Rohling, E.J., Grant, K., van der Meer, M.T.J., Schouten,
1531 S., Baranowski, U., Kucera, M., 2011. Sensitivity of Red Sea circulation to sea level
1532 and insolation forcing during the last interglacial. *Climate of the Past* 7, 941-955. □
1533

1534 UN-ESCWA and BGR (United Nations Economic and Social Commission for
1535 Western Asia; Bundesanstalt für Geowissenschaften und Rohstoffe). 2013. Inventory
1536 of Shared Water Resources in Western Asia. Beirut.
1537

1538 Vaks, A., Bar-Matthews, M., Matthews, A., Ayalon, A., Frumkin, A., 2010. Middle-
1539 Late Quaternary paleoclimate of northern margins of the Saharan-Arabian Desert:
1540 reconstruction from speleothems of Negev Desert, Israel. *Quaternary Science
1541 Reviews* 29, 2647-2662.
1542

1543 Vincent, P., 2008. Saudi Arabia An Environmental Overview, London, Taylor &
1544 Francis Group
1545
1546 Wagner, W., 2011. Groundwater in the Arab Middle East. Springer Science &
1547 Business Media.
1548
1549 Waldmann, N., Torfstein, A., Stein, M., 2010. Northward intrusions of low- and mid-
1550 latitude storms across the Saharo-Arabian belt during past interglacials. *Geology* 38
1551 (6), 567-570.
1552
1553 Whitney, J.W., Gettings, M.E., 1982. Preliminary Geological Investigation of the Bir
1554 Hayzan Diatomite Deposit, Kingdom of Saudi Arabia. USGS Open-File Report - OF-
1555 02-7. Saudi Arabian Deputy Ministry for Mineral Resources, Riyadh.
1556
1557 Whitney, J.W., Faulkender, D.J., Rubin, M., 1983. The Environmental History and
1558 Present Condition of Saudi Arabia's Northern Sand Seas. USGS Open-File Report.
1559 Saudi Arabian Deputy Ministry for Mineral Resources, Riyadh.
1560
1561 Williams, M.A.J., Duller, G.A.T., Williams, F.M., Woodward, C.J., Macklin, M.G.,
1562 El Tom, O.A.M., Munro, R.N., El Hajaz, Y., Barrows, T.T., 2015. Causal links
1563 between Nile floods and eastern Mediterranean sapropel formation during the past
1564 125 kyr confirmed by OSL and radiocarbon dating of Blue and White Nile sediments.
1565 *Quaternary Science Reviews* 130, 89–108
1566
1567 Wood, W.W. and Osterkamp, W.R., 1987. Playa-lake basins on the Southern High
1568 Plains of Texas and New Mexico: Part II. A hydrologic model and mass-balance

1569 arguments for their development. Geological Society of America Bulletin, 99(2), 224-
1570 230.

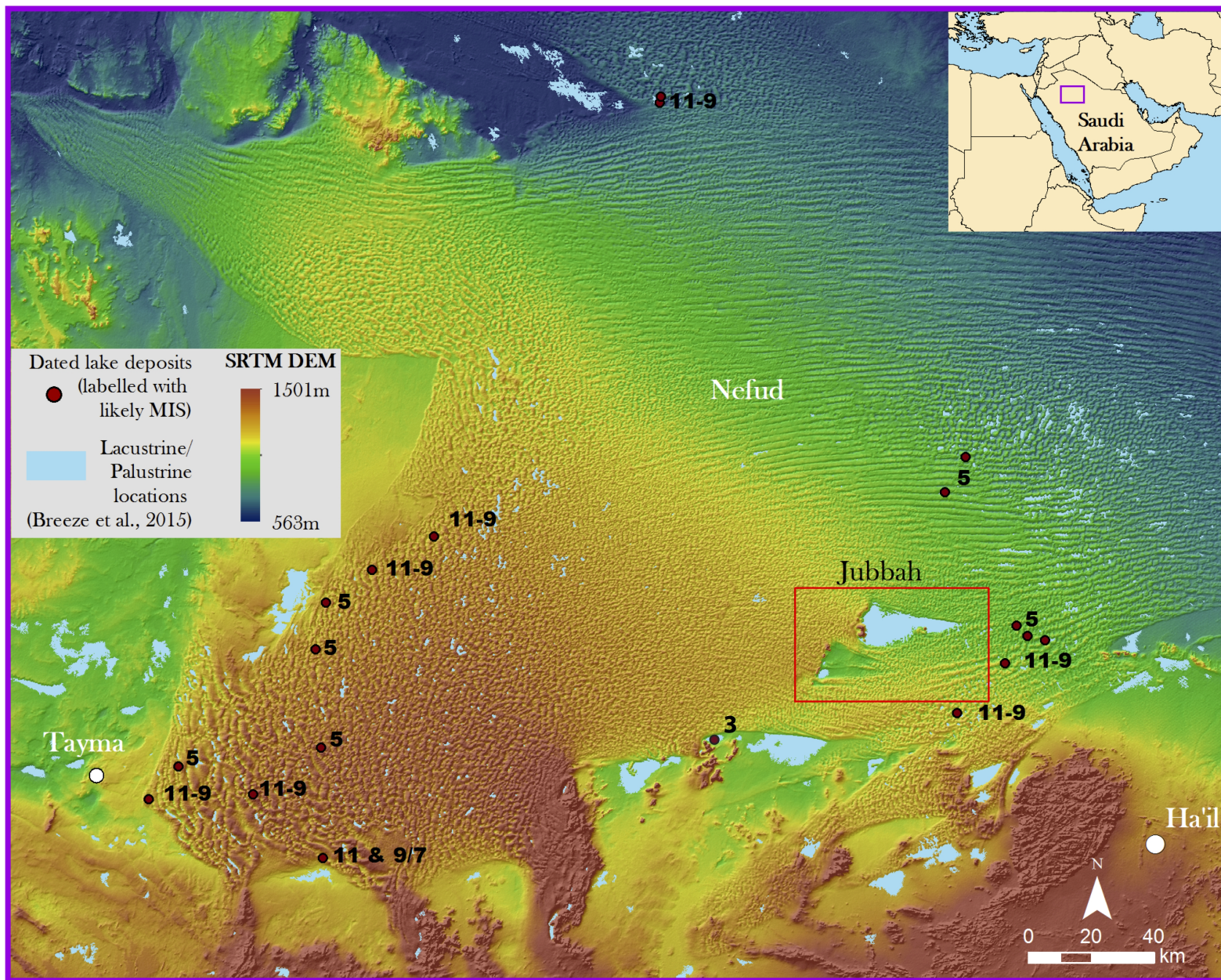
1571

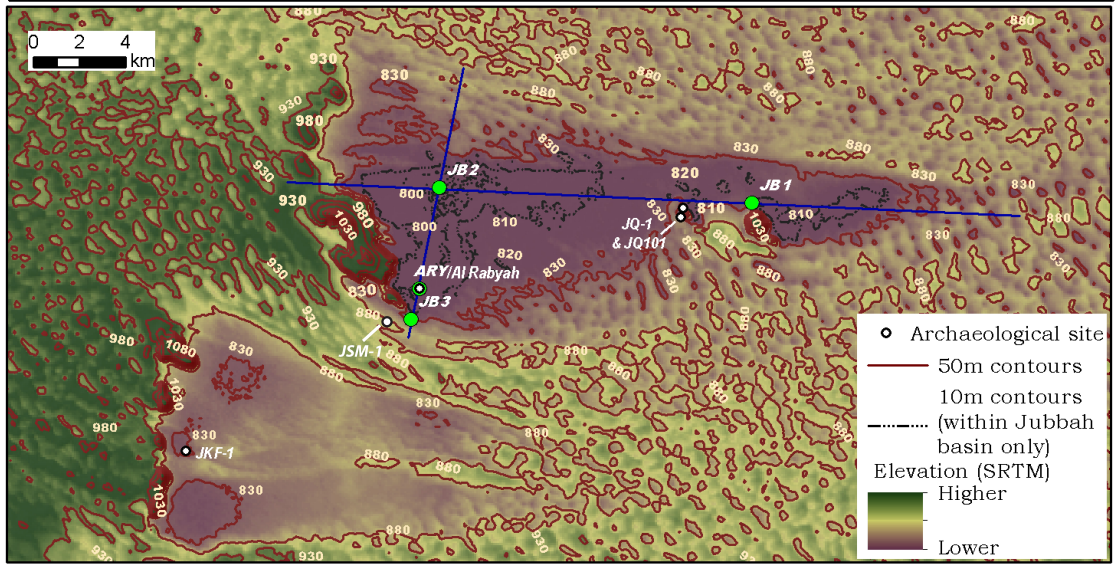
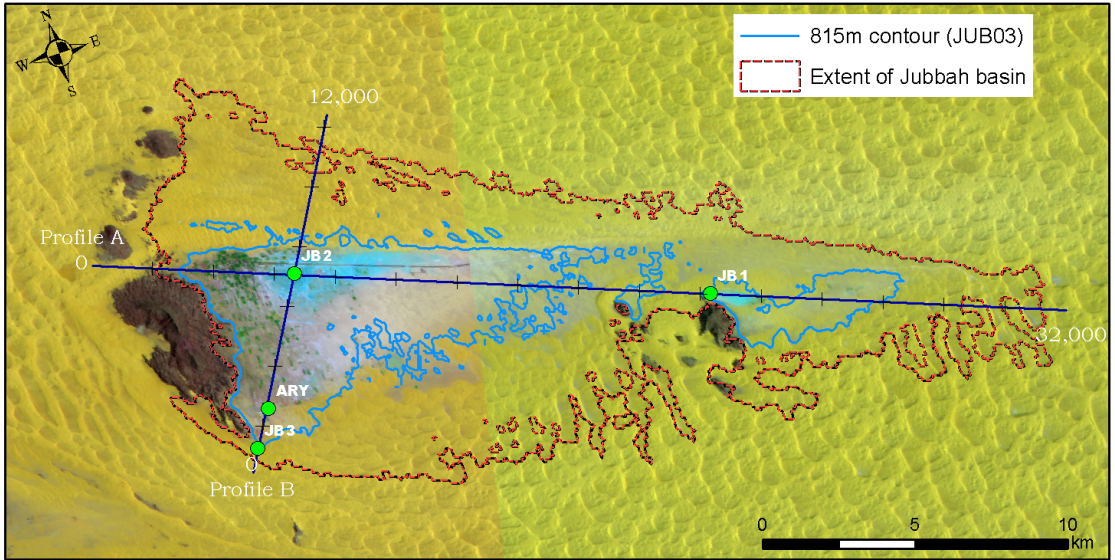
1572 Wood, W.W., Rizk, Z.S., Alsharhan, A.S., 2003. Timing of recharge, and the origin,
1573 evolution, and distribution of solutes in a hyperarid aquifer system. In: Alsharhan,
1574 A.S., Wood, W.W. (Eds.), Water Resources Perspectives: Evaluation Management
1575 and Policy. Elsevier, Amsterdam, pp. 295-312.

1576

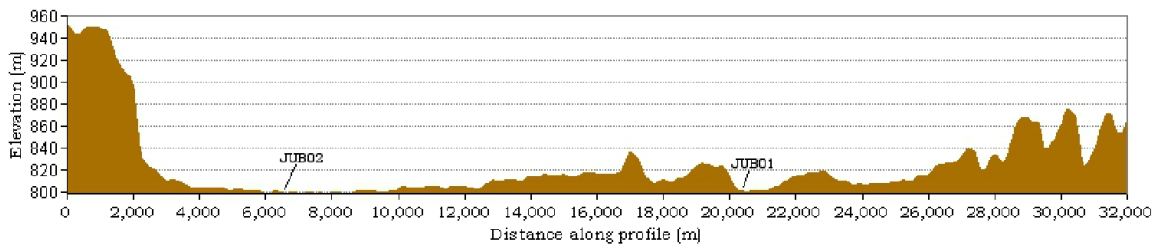
1577

1578

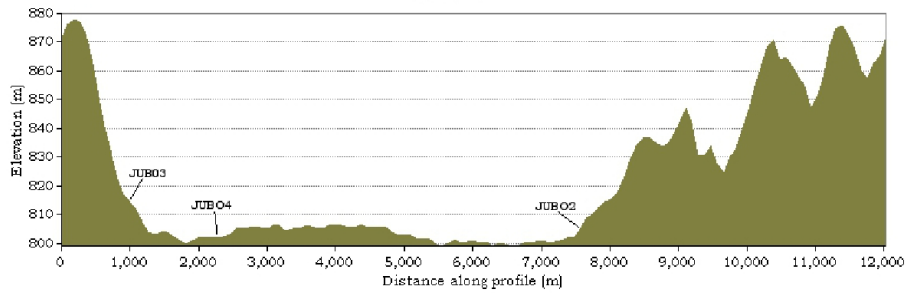




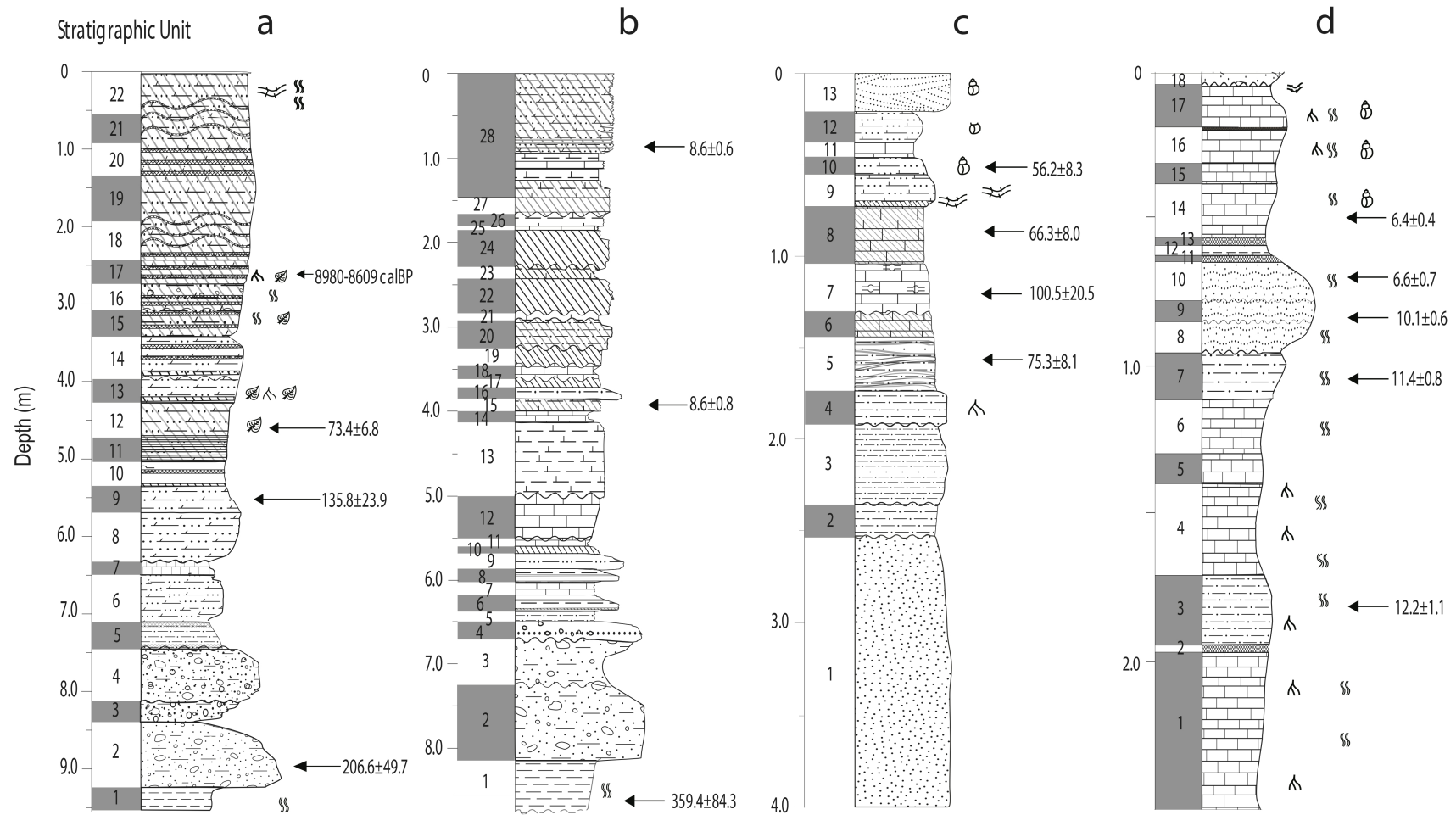
Profile A



Profile B

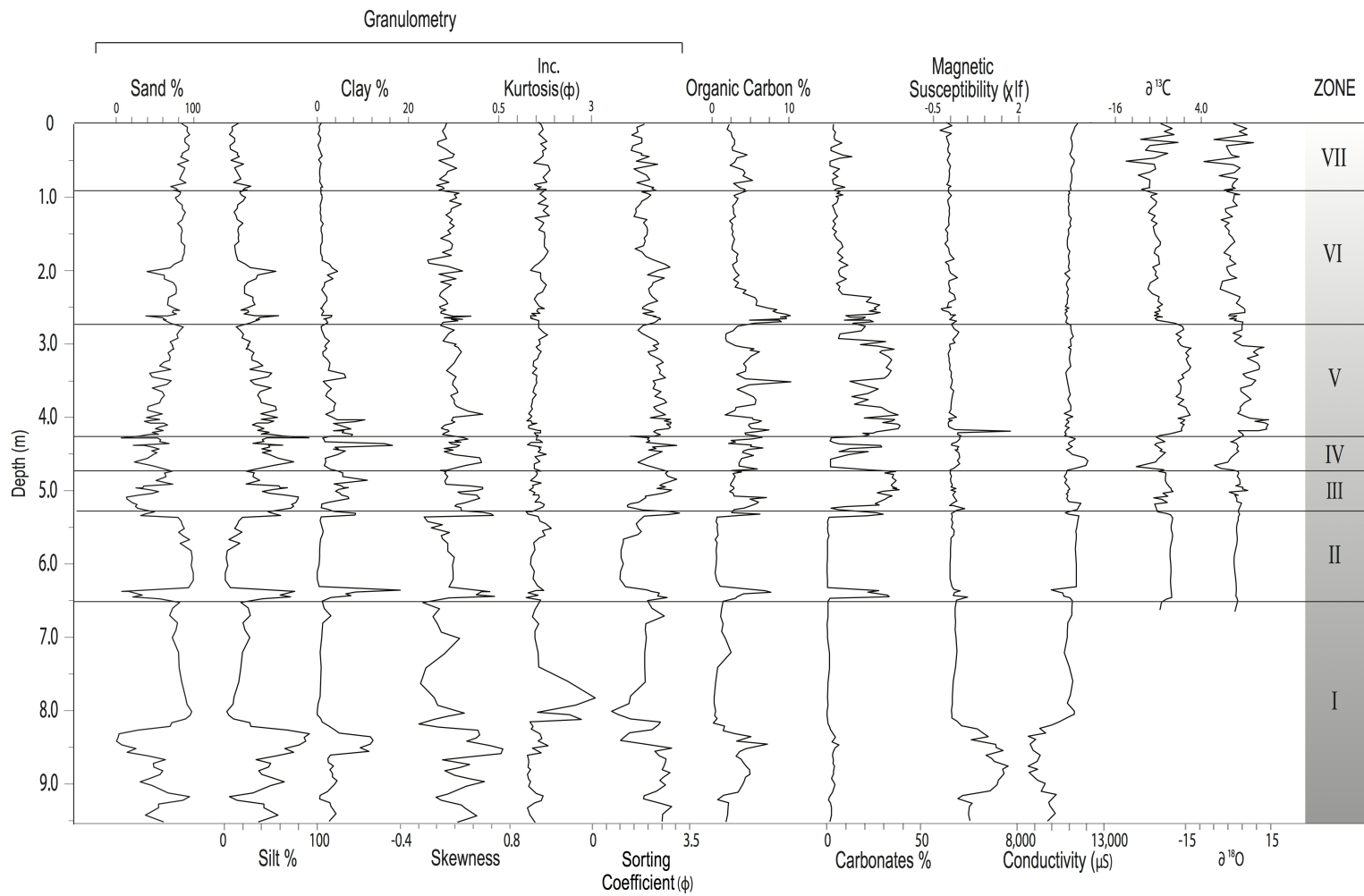


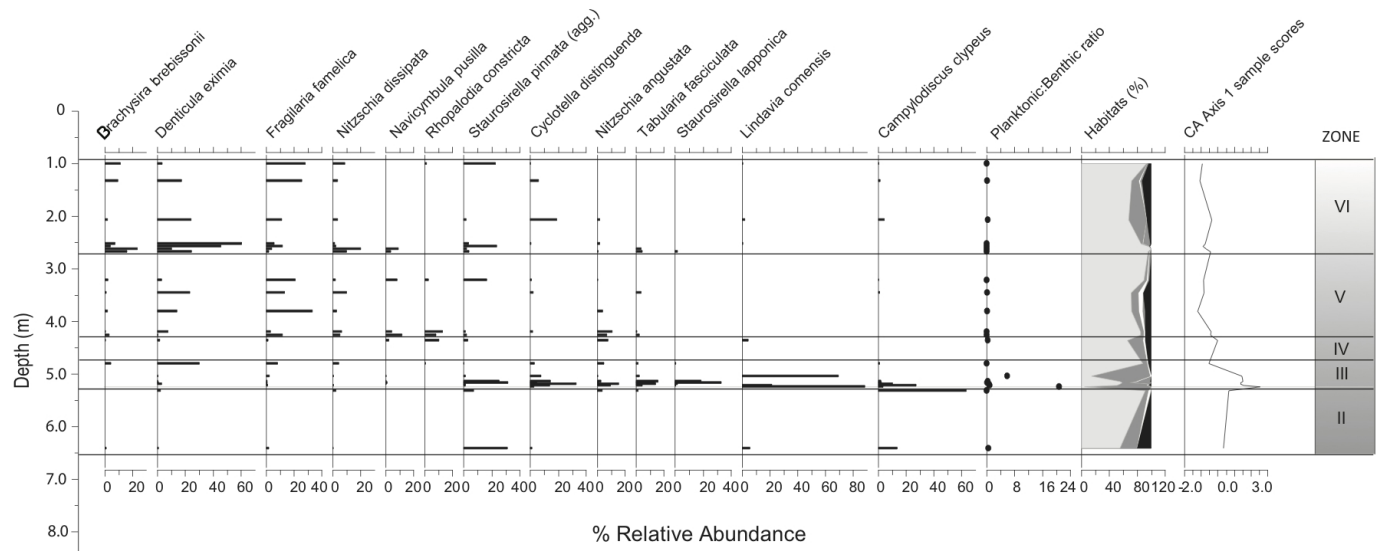




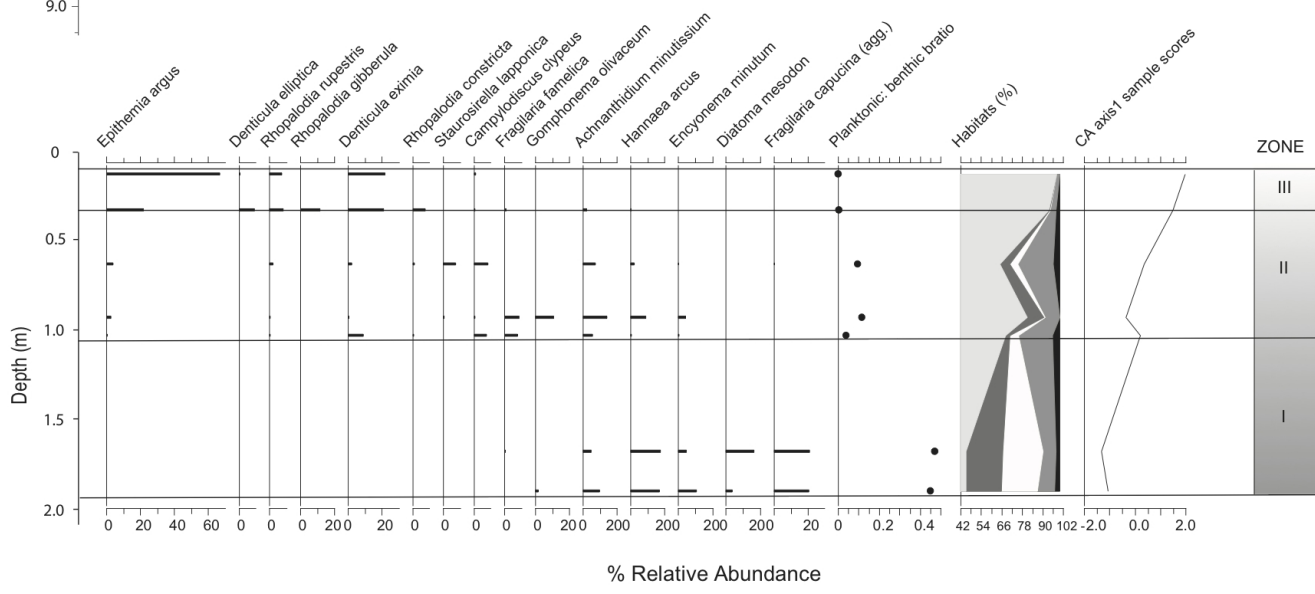
Lithology





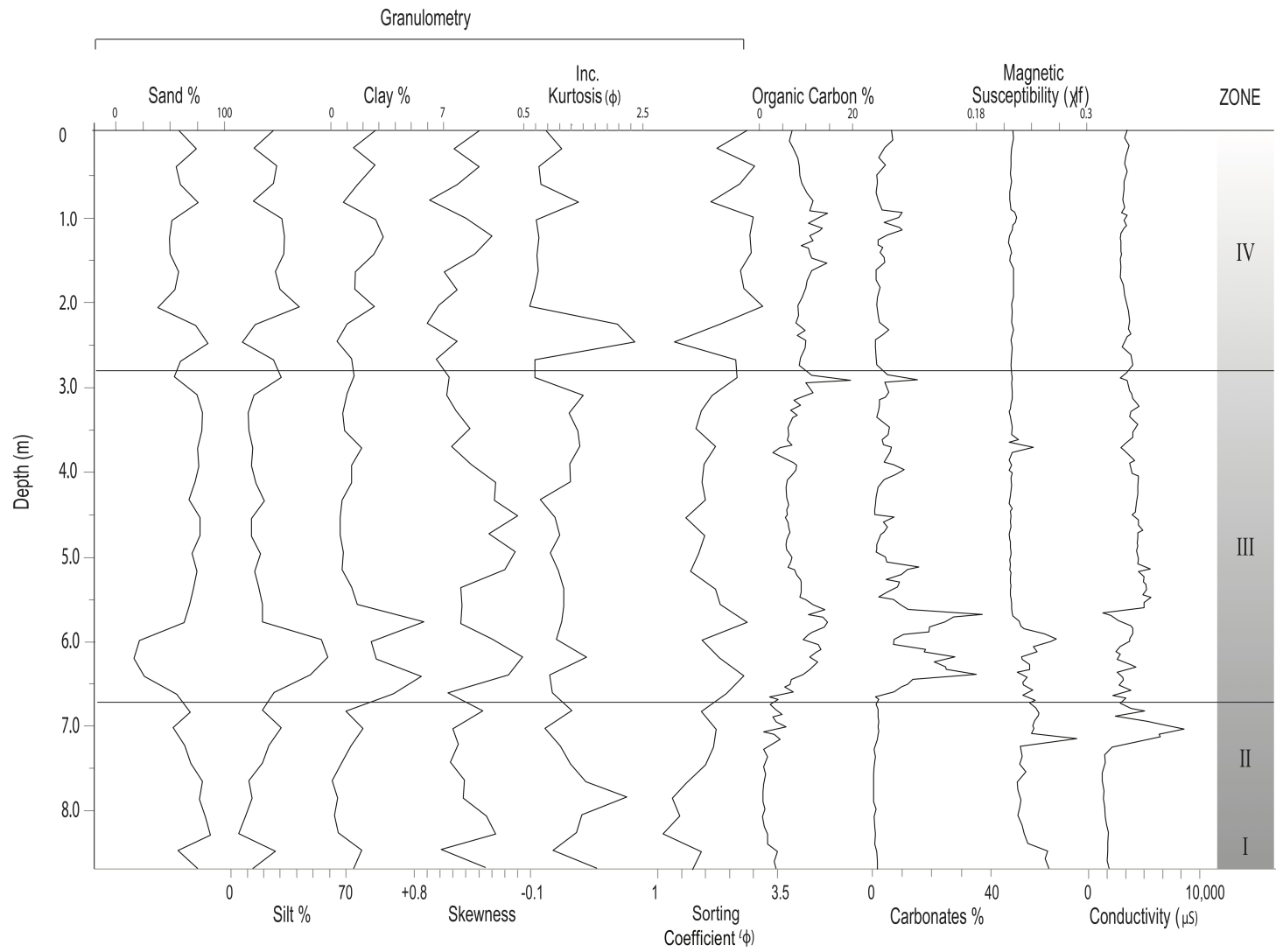


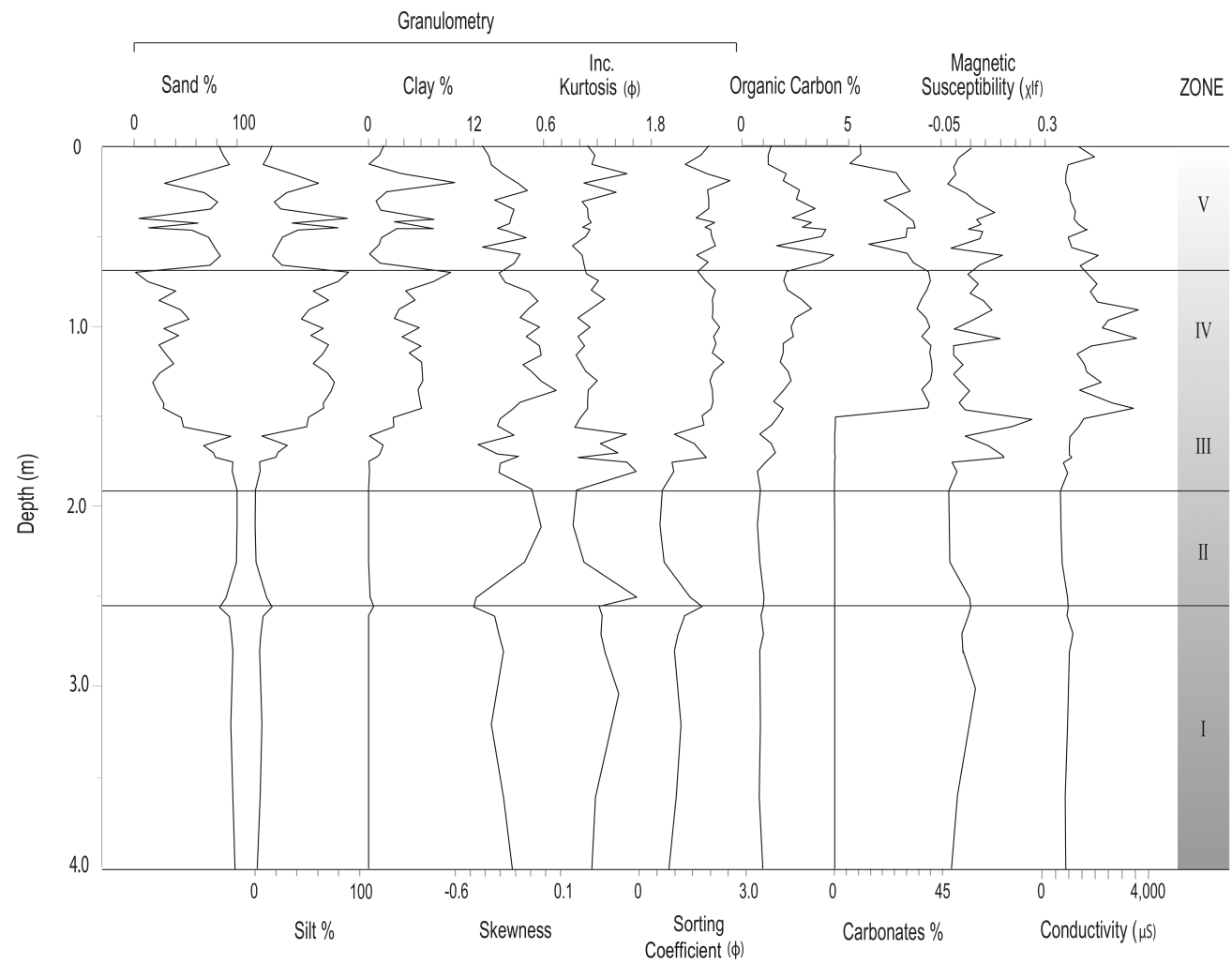
a

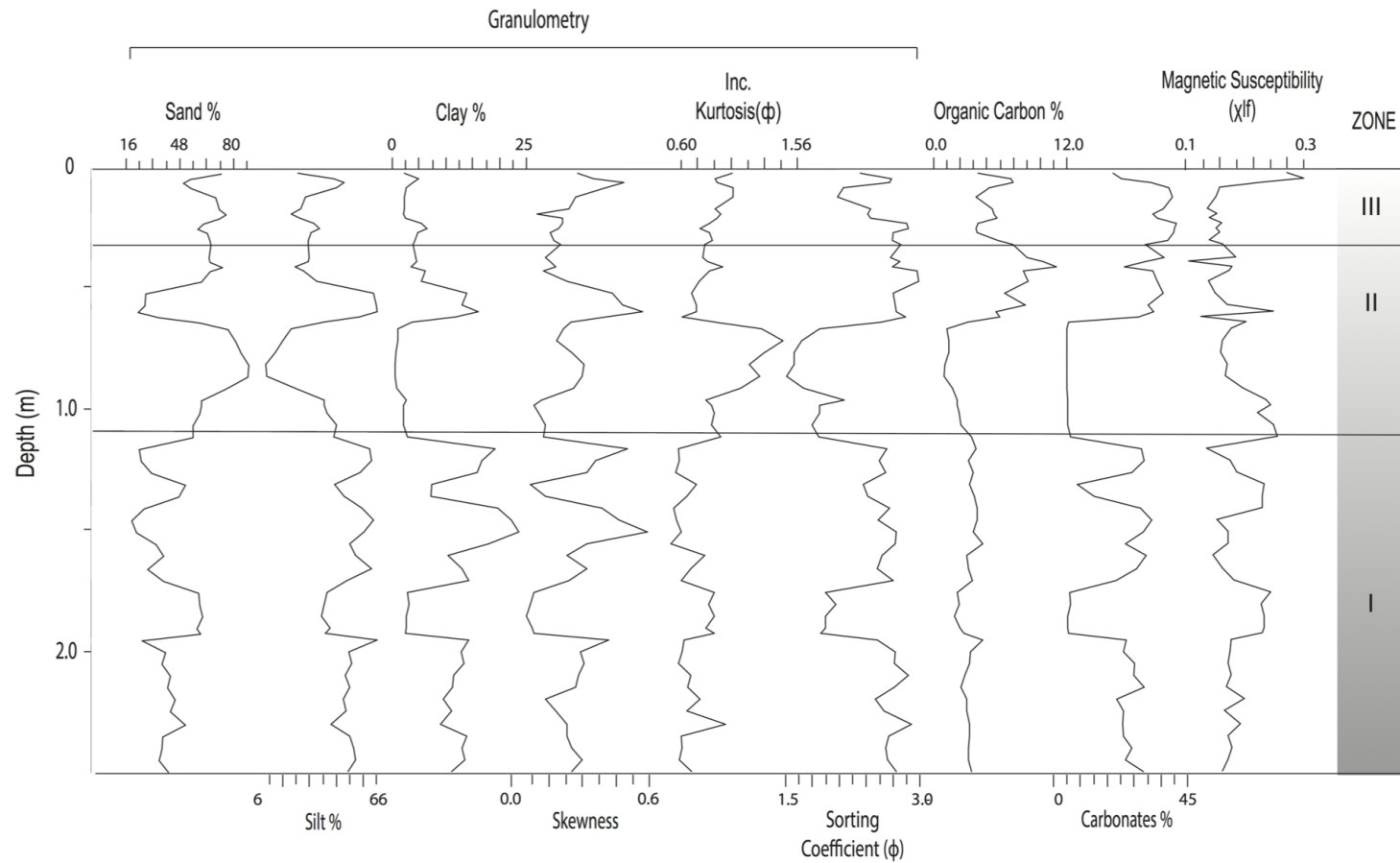


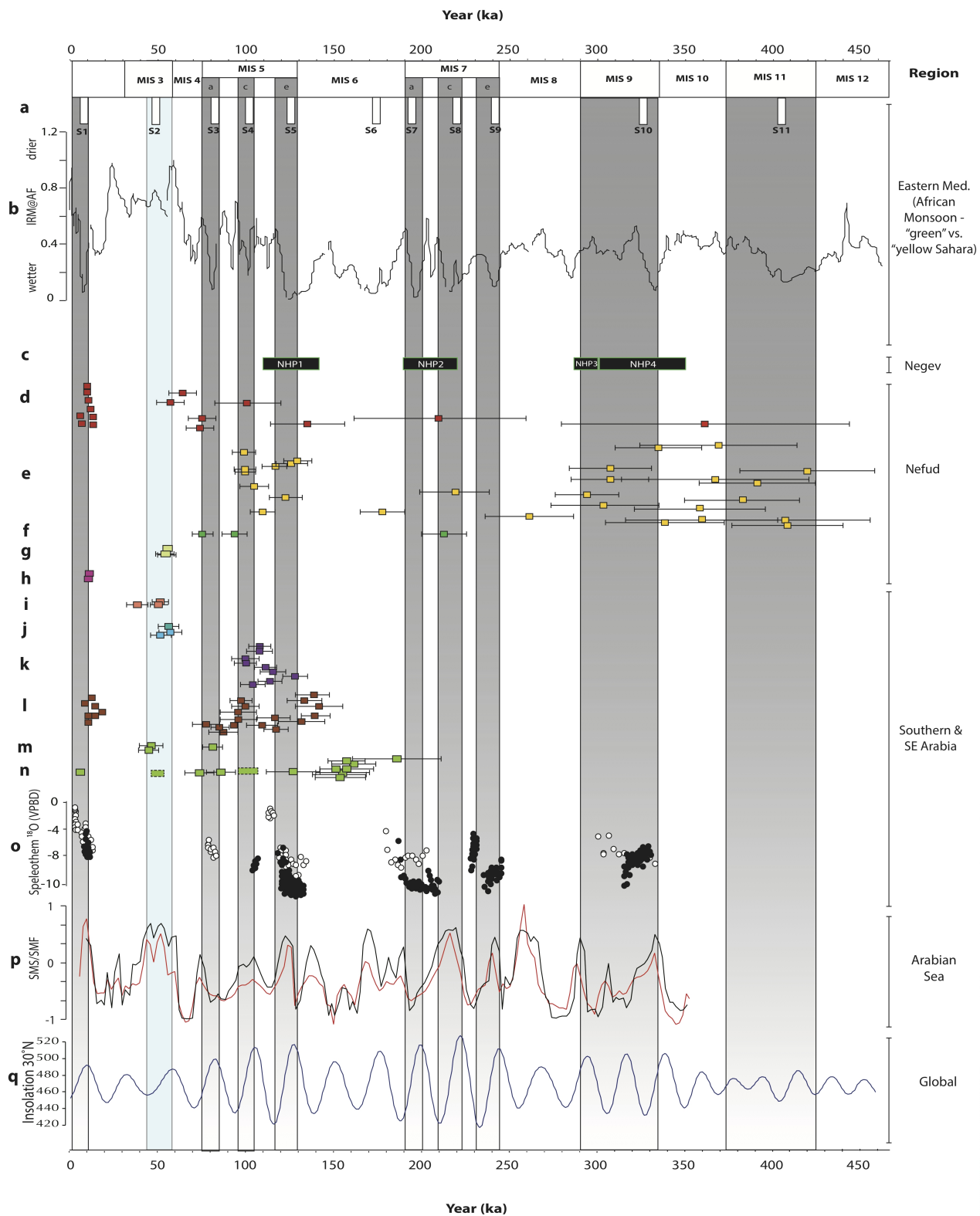
b

- Habitat classifications
- Benthic
 - Planktonic
 - Tycho planktonic
 - Periphytic
 - Epipelagic
 - Unknown









Field Code	Lab Code	Depth (m)	Mineral	Measured (# aliquots)	Accepted (# aliquots)	Overdispersion (%)	D _e (Gy)	D _r (Gy ka ⁻¹)	Age (ka)
ARY-OSL4	X6141	0.45	Q	15	14	19.21 ± 4.00	9.22 ± 0.50	1.44 ± 0.05	6.4 ± 0.4
JB1-OSL5	X 6250	4.51	F	10	10	19.43 ± 6.79	357.06 ± 28.46	4.86 ± 0.23	73.4 ± 6.8
JB1-OSL8	X 6253	5.50	F	10	8	43.49 ± 11.9	302.45 ± 48.79	2.23 ± 0.16	135.8 ± 23.9
JB1-OSL13	X 6258	9.00	F	10	5	47.96 ± 18.18	889.16 ± 209.98	4.30 ± 0.20	206.6 ± 49.7
JB2-OSL1	X 6216	0.77	Q	18	12	14.43 ± 4.62	5.93 ± 0.32	0.69 ± 0.03	8.6 ± 0.6
JB2-OSL4	X 6219	3.94	Q	20	7	18.24 ± 6.62	9.78 ± 6.62	1.14 ± 0.05	8.6 ± 0.8
JB2-OSL14	X 6228	8.65	F	8	6	54.11 ± 16.17	844.81 ± 189.89	2.35 ± 0.16	359.4 ± 84.3
JB3-OSL1	X 6231	1.20	Q	18	14	52.18 ± 10.31	61.63 ± 8.79	1.10 ± 0.04	56.2 ± 8.3
JB3-OSL2	X 6232	1.67	Q	18	14	48.08 ± 9.90	55.00 ± 6.32	0.83 ± 0.03	66.3 ± 8.0
JB3-OSL3	X 6233	2.07	Q	18	10	62.22 ± 14.42	83.60 ± 16.75	0.83 ± 0.03	100.5 ± 20.5
JB3-OSL4	X 6234	2.50	Q	18	11	30.83 ± 7.77	94.98 ± 9.64	1.26 ± 0.05	75.3 ± 8.1